

Asymptotic behavior of the Sudakov form factor in quantum chromodynamics

Ashoke Sen

Institute for Theoretical Physics, State University of New York at Stony Brook, Stony Brook, New York 11794

(Received 15 May 1981)

In this paper we give an algorithm to compute the asymptotic behavior of the on-shell quark form factor in the limit of large momentum transfer (Sudakov form factor) in Abelian and non-Abelian gauge theories. We ignore terms which are suppressed by a power of momentum transfer, but keep all nonleading logarithms of the momentum transfer and all powers of the coupling constant.

I. INTRODUCTION

In this paper we shall give a systematic procedure for computing the asymptotic behavior of the on-shell quark electromagnetic form factor in non-Abelian gauge theories. In our calculation we sum up all the terms in perturbation series of order $(g^2)^\nu [\ln(q^2/m^2)]^\nu$ ($\nu \leq 2n$) but ignore terms of order $m/(q^2)^{1/2}$, where q^2 , m , and g are the four-momentum squared of the external photon, mass of the quark, and the coupling constant, respectively. Calculation of asymptotic form factors in gauge theories began with the pioneering work of Sudakov¹ who calculated the asymptotic fermion form factor in QED by summing up the leading-logarithmic terms. Since such form factors are infrared divergent, Sudakov regulated the divergence by keeping the external particles off shell by a fixed amount. In his calculation Sudakov found that the form factor exponentiates in a form $\exp[-(g^2/8\pi^2) \ln(|q^2|/m_a^2) \ln(|q^2|/m_b^2)]$, m_a^2 and m_b^2 being the invariant mass squared of the external fermions. Jackiw² and Fishbane and Sullivan³ repeated his calculation but this time regulating the infrared divergence by giving the photon a small mass m_{ph} , the external fermions being put on shell. They calculated the amplitude in leading-logarithmic approximation and found that the form factor exponentiates in the form

$$\exp\left(-\frac{g^2}{16\pi^2} \ln^2 \frac{|q^2|}{m_{ph}^2}\right).$$

The functional forms given above are rapidly decaying functions of q^2 in the limit $|q^2| \rightarrow \infty$ and hence one may expect that the nonleading logarithms or even the terms which are suppressed by a power of $|q^2|$ may add up to give a contribution which completely upsets the leading-logarithmic result. Progress has been made in order to sum up such terms. It has been shown by Mueller⁴ and by Collins⁵ that in QED the nonleading logarithms also sum up to give a decreasing exponential and hence do not upset the leading-logarithmic result. In their analysis they have in-

cluded all terms of order $(g^2)^\nu [\ln(q^2/m^2)]^\nu$ but ignored terms which are suppressed by a power of $|q^2|$ order by order in perturbation theory.

Attempts have also been made to calculate the electromagnetic form factor of quarks in non-Abelian gauge theories. It was shown by Cornwall and Tiktopoulos⁶ that both the Sudakov as well as the on-shell quark form factors exponentiate up to three-loop order in the leading-logarithmic approximation. This has been verified up to all orders in leading-logarithmic approximation by Dalman and Steiner⁷ and by Belokurov and Ussyukina.⁸ Attempts have been made to extend this proof for nonleading logarithms as well⁹ without complete success.

In this paper we shall give an algorithm to compute the on-shell singlet quark form factor in non-Abelian gauge theories which includes leading as well as nonleading logarithms using a somewhat similar approach as Ref. 5. It is found that the nonleading logarithms also add up to give a decreasing exponential and hence do not upset the leading-logarithmic result. In order to control the infrared divergence we may either give the gluons a small mass m_g and consistently ignore all terms of order m_g that appear in perturbation theory calculation (in order to maintain gauge invariance) or we may use the technique of dimensional regularization to control the infrared divergences of the theory.¹⁰ In whatever way the infrared divergences are regulated, we call the infrared regulator τ . The $\tau \rightarrow 0$ limit corresponds to the infrared-divergent point. The external quarks are put on shell. Thus the limit we are considering is identical to the limit considered by Jackiw² and Fishbane and Sullivan³ rather than the one used by Sudakov.¹ We shall, however, still refer to the form factor as the Sudakov form factor in later sections.

The form factor is infrared divergent, as are all on-shell QCD amplitudes. But we are interested in the asymptotic behavior of the form factor and we shall study this by giving the infrared regulator τ a small but fixed value. If we sum

over soft-gluon emission then the infrared divergence will cancel¹¹ and presumably the asymptotic behavior of the form factor will still be given by the expression derived in this paper, with τ replaced by the energy resolution ϵ of the detector.

For removing the ultraviolet divergence we may use the minimal-subtraction scheme in dimensional renormalization.¹² However, for reasons to become clear later it will be more convenient to choose the renormalized mass m_R of the quark to be equal to its physical mass m . We shall keep our discussion general by denoting the renormalized and physical masses of the quark by different symbols. In Sec. IV we shall find the simplification that occurs by taking m_R to be equal to m . The other counterterms are fixed by the usual minimal-subtraction scheme.

We choose to work in the axial gauge where we can use the power-counting techniques and results of Sterman¹³ to identify the regions in loop momentum space which may contribute to the form factor in leading power in $|q^2|$. For definiteness we shall consider the case where a timelike photon with large invariant mass decays into a quark-antiquark pair moving in the + and - z direction, respectively, with momentum p and p' . The analysis however remains true for the scattering of a quark by a spacelike photon with large negative momentum squared. An internal line carrying momentum k may belong to any of the following categories: (1) Contracted: if $|k^\mu| \gtrsim (q^2)^{1/2}$ for every μ , (2) collinear to p : $|k^+| \sim p^+$, $|k^-| \sim \lambda p^+$, $|k_\perp| \sim \lambda^{1/2} p^+$ with $\lambda \rightarrow 0$, (3) collinear to p' : $|k^-| \sim p'^-$, $|k^+| \sim \lambda p'^-$, $|k_\perp| \sim \lambda^{1/2} p'^-$ with $\lambda \rightarrow 0$, or (4) soft: $|k^\mu| \sim \lambda (q^2)^{1/2}$ for every μ with $\lambda \rightarrow 0$.

Any region in momentum space which contributes to the Sudakov form factor in leading power in q^2 will correspond to the following picture according to Ref. 13. The incoming photon will break up into a $q\bar{q}$ pair through a (contracted) three-point vertex moving parallel to p and p' , respectively. This quark (antiquark) may decay into other particles moving parallel to it thus producing a jet of particles moving parallel to p (p'). The lines in a jet may interact with each other or with lines in the other jet through soft-gluon exchange. Finally all the lines in the jet moving parallel to p (p') must combine to produce the external quark (antiquark). The following rules must be satisfied. (a) A soft gluon may interact with a jet only through a (contracted) three-point vertex. (b) Jet lines belonging to the same jet may interact with each other through (contracted) three- or four-point vertices.

Note that there may be other regions in momentum space which may give a logarithmically divergent contribution by naive power counting but the

contours of integration are not pinched.¹³ For example, if a soft gluon of momentum k is exchanged between the two jets, we may get a logarithmically divergent contribution from the region where k^+ or k^- or both are small compared to k_\perp ; however, such regions are not pinched. We do not have to analyze the contribution from such regions, since although the integrand may show singularities, the integral will not receive any singular contribution from such regions.

We start with simple ladder diagrams since they do not have any collinear divergences associated with them. In Sec. III we show how the contribution from such diagrams may be brought into a simple exponential form. This is done by considering the effect of the operation of $\partial/\partial \ln(q^2)^{1/2}$ on a Feynman diagram, which helps us in forming a differential equation involving the total contribution from the ladder diagrams. This technique however cannot be applied to a general Feynman diagram which involves collinear as well as soft divergences. In Sec. IV using the Grammer-Yennie decomposition technique¹⁴ we show how to bring the total contribution from all Feynman diagrams into a form where the only lines parallel to p are those in the self-energy insertion on the external quark line. The rest of the diagram does not contain any line parallel to p and may be analyzed by the technique of Sec. III. The double-logarithmic contributions however remain in the self-energy insertions on external lines. We show in Sec. V that the constraint that the final result must be Lorentz covariant and the results of Sec. IV are sufficient to show that the contributions from the self-energy graphs also exponentiate. We could have stopped at this stage but in Sec. VI we give a more direct analysis of self-energy graphs in which we study the change in the self-energy graphs under an infinitesimal boost in the z direction. This helps in forming a differential equation involving wave-function renormalization constants, the solution to which gives the required exponential form of the fermion self-energy. Our final result is given in Eq. (6.33) and the asymptotic behavior of the form factor in the limit $q^2 \rightarrow \infty$ is given in Eq. (6.42). Appendix A describes various special vertices that we shall use in the text. Appendix B deals with a problem discussed in the text which appears due to the presence of special composite three-point vertices. Appendix C describes a special gluon propagator discussed in the text.

The analysis of form factor given in this paper may be applied to QED also. In this case the factorization of the soft divergences from the collinear divergences is much simpler (see Ref. 5). As a result the analysis of Sec. IV will be much

simpler. The rest of the analysis may be carried out in the same way. This is a considerable simplification of the treatment of QED form factor in Ref. 5.

Some of the techniques used in this paper (particularly those used in Sec. VI) were found independently by Collins and Soper¹⁵ in their analysis of back-to-back jets in QCD.

II. KINEMATICS AND SOME CONVENTIONS

For definiteness we shall consider the amplitude where an incoming timelike photon with large invariant mass decays into a quark-antiquark pair. We shall work in a frame where the momentum of the incoming photon, momentum of the outgoing quark, and that of the outgoing antiquark have, respectively, the form

$$\begin{aligned} q &= (Q \cosh\beta, 0, 0, Q \sinh\beta), \\ p &= \left(\frac{Q}{2} \cosh\beta + \left(\frac{Q^2}{4} - m^2 \right)^{1/2} \sinh\beta, 0, 0, \left(\frac{Q^2}{4} - m^2 \right)^{1/2} \cosh\beta + \frac{Q}{2} \sinh\beta \right), \\ p' &= \left(\frac{Q}{2} \cosh\beta - \left(\frac{Q^2}{4} - m^2 \right)^{1/2} \sinh\beta, 0, 0, - \left(\frac{Q^2}{4} - m^2 \right)^{1/2} \cosh\beta + \frac{Q}{2} \sinh\beta \right), \end{aligned} \quad (2.1)$$

where β is a finite number. In most of our calculations we shall take β to be zero except in Sec. V where we take p and p' to be independent variables. Here m is the physical mass of the quark. Let us denote the renormalized mass of the quark by m_R and the renormalization mass by μ .

We choose to work in the axial gauge where the gluon propagator has the form

$$(-i) N_{ab}^{\mu\nu}(k)/(k^2 + i\epsilon) = \delta_{ab} [(-i)/(k^2 + i\epsilon)] [g^{\mu\nu} - (k^\mu n^\nu + k^\nu n^\mu)P(1/k \cdot n) + k^\mu k^\nu P(1/k \cdot n)^2 n^2], \quad (2.2)$$

where

$$P(1/k \cdot n)^\alpha = \lim_{\epsilon \rightarrow 0} [1/(k \cdot n + i\epsilon)^\alpha + 1/(k \cdot n - i\epsilon)^\alpha] / 2 \quad (2.3)$$

and n is a spacelike vector. In Eq. (2.2) μ, ν are the Lorentz indices and a, b are the group indices. For reasons that will become clear later we choose n_\perp to be proportional to ϵ , the polarization of the external photon. Other components of n are arbitrary ($n_3 \neq 0$).

For any four-vector k we define the light-cone coordinates as

$$k^* = k^0 \pm k^3, \quad k_\perp = k_T = (0, k_1, k_2, 0). \quad (2.4)$$

For later convenience we shall fix up some conventions. Whenever we draw a Feynman diagram we shall draw the incoming particles to the left and the outgoing particles to the right and refer to left and right side of the diagram according to this convention. In any Feynman diagram contributing to the Sudakov form factor we may identify the fermion line which is contracted with the quark and the antiquark wave function at its two extreme ends. The part of this line lying between the external quark and the point where the incoming photon meets this line will be referred to as the outgoing quark line; the other part will be referred to as the outgoing antiquark line. If the incoming photon breaks up into a number of gluons through fermion loops before meeting this line (as in Fig. 1), then we choose right-most points (P and P') where these gluons meet the fermion line and the parts of the fermion line lying to the right of these

points will be called outgoing quark and antiquark lines, respectively.

In order to calculate the Sudakov form factor we shall evaluate the sum of all Feynman diagrams including self-energy insertions on external lines. If we call the sum of all such diagrams $G(p, p')$, then the Sudakov form factor is given by

$$\bar{u}(p)(\not{p} - m)[Z_2(p)]^{-1/2} G(p, p')[Z_2(p')]^{-1/2} (\not{p}' - m)v(p'). \quad (2.5)$$

where $[Z_2(p)]^{1/2}$ and $[Z_2(p')]^{1/2}$ are the external wave-function renormalization factors (finite).

In any figure a four-gluon vertex will be indicated by a dot in order to distinguish it from a figure with two gluon lines crossing each other.

III. EXPONENTIATION OF LADDER DIAGRAMS

We shall first explain the exponentiation technique with the help of ladder diagrams. These dia-

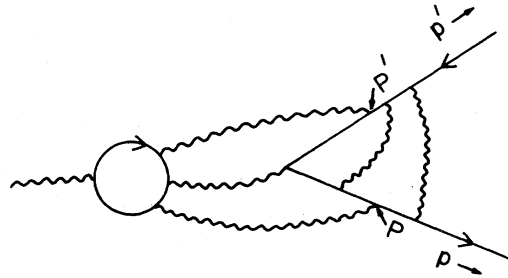


FIG. 1. A typical diagram contributing to the Sudakov form factor.

grams are easy to analyze since they do not have any collinear divergence. A typical ladder diagram is shown in Fig. 2. Let $F(k, k')$ be the quark-antiquark-quark-antiquark Green's function with the incoming quark (antiquark) carrying momentum $p+k$ ($p'-k$) and the outgoing quark (antiquark) carrying momentum $p+k'$ ($p'-k'$), respectively. F includes two-particle reducible as well as two-particle irreducible Green's functions containing ladder diagrams only. It includes the propagators of the incoming lines but not those of the outgoing lines. Color and Dirac indices of F are understood. Then, if we denote by Γ the contribution to the Sudakov form factor from ladder diagrams only, we may write

$$\Gamma(p, p') = \int \frac{d^4k}{(2\pi)^4} \epsilon \cdot \gamma F(k, 0), \quad (3.1)$$

ϵ being the polarization vector carried by the external photon. We shall deal with the case where ϵ corresponds to transverse polarization, since the form factor for a longitudinally polarized incoming photon is suppressed³ [by a power of $(q^2)^{1/2}$]. The right-hand side of Eq. (3.1) has been explained in Fig. 3.

Let us denote by $K(k, k')$ the two-particle irreducible connected Green's function for $q\bar{q} \rightarrow q\bar{q}$, which again includes the propagators corresponding to the incoming lines but not those corresponding to the outgoing lines. Then we may write

$$F(k, k') = (2\pi)^4 \delta^{(4)}(k - k') + \int K(k, k'') F(k'', k') \frac{d^4k''}{(2\pi)^4}. \quad (3.2)$$

This equation is shown in Fig. 4.

Let us now consider the effect of applying the $\partial/\partial \ln Q$ operator on Γ where $Q = (q^2)^{1/2}$. Γ is expressed as a Feynman integral where the momenta of the internal gluons are treated as independent loop momenta. As a result the only dependence of Γ on Q comes from the dependence of the momenta of the internal fermion lines on p and p' , which may be written as $p+K$ or $p'-K'$, K (K') being some linear combination of the internal gluon momenta. Then we may write

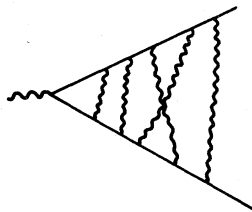


FIG. 2. A typical ladder diagram.

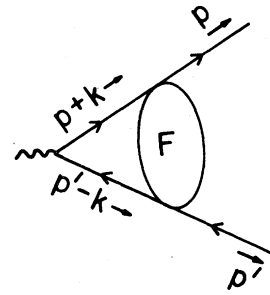


FIG. 3. Graphical representation of the right-hand side of Eq. (3.1).

$$\frac{\partial \Gamma}{\partial \ln Q} = \frac{\partial \Gamma}{\partial \ln p^+} + \frac{\partial \Gamma}{\partial \ln p'^-}, \quad (3.3)$$

where in $\partial \Gamma/\partial \ln p^+$ the derivative operator acts on lines carrying momenta $p+K$ and in $\partial \Gamma/\partial \ln p'^-$ the derivative operator acts on lines carrying momenta $p'-K'$. Equation (3.3) was based on the fact that

$$\partial \ln p^+ / \partial \ln Q \approx 1 \approx \partial \ln p'^- / \partial \ln Q. \quad (3.4)$$

Let us denote the derivative operation by putting a cross on the fermion line. Thus the right-hand side of Eq. (3.3) is given by the sum of all Feynman diagrams one of whose internal fermion line is crossed.

Now if the momentum K is soft then the contribution from the line carrying momentum $p+K$ must go as $p^* \gamma^- / [(p+K)^2 - m^2 + i\epsilon] \approx p^* \gamma^- / (p^* K^- + i\epsilon) \approx \gamma^- / (K^- + i\epsilon)$ and hence is independent of p^+ . Thus if such a line is crossed we shall get zero contribution from it. In other words a crossed line cannot carry soft momentum from the internal gluons. The only other alternative is that the crossed line must be contracted (since for ladder diagrams K cannot be parallel to p).

Thus we may express $\partial \Gamma/\partial \ln p^+$ as

$$\frac{\partial \Gamma}{\partial \ln p^+} = \int \phi(k) F(k, 0) \frac{d^4k}{(2\pi)^4}, \quad (3.5)$$

where $\phi(k)$ is a vertex function carrying such a cross on the p line that all its internal lines are constrained to be contracted. Typical contributions to $\phi(k)$ have been shown in Fig. 5. Note that in Fig. 5(c) the crossed line constrains both the gluons S_1 and S_2 to be contracted (a result of power

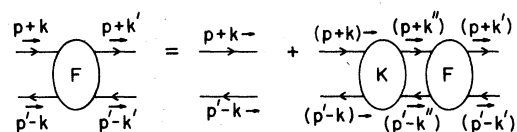
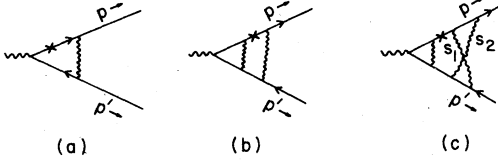


FIG. 4. Diagrammatic representation of Eq. (3.2).

FIG. 5. Typical contributions to $\phi(k)$.

counting). Now if we consider the region of integration where the momentum k in the right-hand side of (3.5) is soft then the part of $\phi(k)$ that contributes to the integral in leading power in p^* must be proportional to a transverse γ matrix since if it is proportional to γ^- we cannot have $p^*\gamma^-$ on the quark line numerator external to ϕ , while if it is proportional to γ^+ we cannot have $p^*\gamma^+$ on the anti-quark line external to ϕ . By rotational invariance this must be proportional to $\epsilon \cdot \gamma$ or $n_1 \cdot \gamma$ (and n_1 has been chosen proportional to ϵ). It will also be independent of k in the limit $|k^\mu| \ll (q^2)^{1/2}$ since all the internal lines of ϕ carry off-shell momenta $\sim (q^2)^{1/2}$. Let us call it $\epsilon \cdot \gamma \chi_0$. χ_0 is a function of $(q^2)^{1/2}$, renormalization mass μ , and the coupling constant g . Thus we may write (3.5) as

$$\begin{aligned} \partial \Gamma / \partial \ln p^* &= \int \chi_0 \epsilon \cdot \gamma F(k, 0) \frac{d^4 k}{(2\pi)^4} \\ &+ \int [\phi(k) - \chi_0 \epsilon \cdot \gamma] F(k, 0) \frac{d^4 k}{(2\pi)^4} \\ &= \chi_0 \Gamma + \int [\phi(k) - \chi_0 \epsilon \cdot \gamma] F(k, 0) \frac{d^4 k}{(2\pi)^4}. \end{aligned} \quad (3.6)$$

Note that since $\phi(k)$ is a color singlet, χ_0 is a number. Now, the contribution to the second term on the right-hand side of (3.6) comes only from the region $|k^\mu| \gtrsim (q^2)^{1/2}$ since in the limit $|k^\mu| \ll (q^2)^{1/2}$, $\phi(k) - \chi_0 \epsilon \cdot \gamma$ tends to zero. Thus if for $F(k, 0)$ in this term we substitute the right-hand side of Eq. (3.2), the $\delta^4(k)$ term will not contribute and it may be written as

$$\begin{aligned} \int [\phi(k) - \chi_0 \epsilon \cdot \gamma] K(k, k') F(k', 0) \frac{d^4 k}{(2\pi)^4} \frac{d^4 k'}{(2\pi)^4} \\ = \int \phi_1(k') F(k', 0) \frac{d^4 k'}{(2\pi)^4}, \end{aligned} \quad (3.7)$$

where

$$\phi_1(k') = \int [\phi(k) - \chi_0 \epsilon \cdot \gamma] K(k, k') \frac{d^4 k}{(2\pi)^4}. \quad (3.8)$$

The right-hand side of Eq. (3.8) is shown in Fig. 6. Since the contribution to this term comes only from the region $|k^\mu| \sim (q^2)^{1/2}$, all the internal lines in Fig. 6 must carry large off-shell momentum

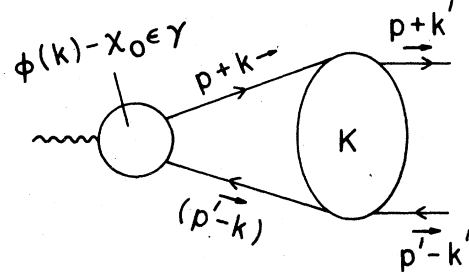


FIG. 6. The right-hand side of Eq. (3.8).

$\sim (q^2)^{1/2}$. As a result we may again decompose $\phi_1(k')$ into $\chi_1 \epsilon \cdot \gamma$ and $\phi_1(k') - \chi_1 \epsilon \cdot \gamma$, such that $\phi_1(k') - \chi_1 \epsilon \cdot \gamma$ does not contribute to the right-hand side of (3.7) for $|k'^\mu| \ll (q^2)^{1/2}$. Like χ_0 , χ_1 is a function of $(q^2)^{1/2}$, μ , and g . We may continue this indefinitely to get an equation, for equation of the form

$$\frac{\partial \Gamma}{\partial \ln p^*} = (\chi_0 + \chi_1 + \dots) \Gamma \equiv \chi \Gamma. \quad (3.9)$$

Similarly we may get

$$\frac{\partial \Gamma}{\partial \ln p'^*} = (\chi'_0 + \chi'_1 + \dots) \Gamma \equiv \chi' \Gamma. \quad (3.10)$$

Thus from (3.3)

$$\frac{\partial \Gamma}{\partial \ln Q} = (\chi + \chi') \Gamma, \quad (3.11)$$

the solution to which is

$$\begin{aligned} \Gamma &= A_0(m, \mu, g, \tau) \\ &\times \exp \left\{ \int^{(q^2)^{1/2}} [\chi(x, \mu, g) + \chi'(x, \mu, g)] \frac{dx}{x} \right\}. \end{aligned} \quad (3.12)$$

Note that since χ and χ' are obtained as sums of diagrams all of whose internal lines carry large off-shell momentum, they are functions of $(q^2)^{1/2}$ and μ but not of the quark mass or the infrared regulator τ . Also since Γ is multiplicatively renormalized, Eq. (3.11) shows that $\chi + \chi'$ is free of ultraviolet divergence. Hence it satisfies the renormalization-group equation

$$\left[\mu \frac{\partial}{\partial \mu} + \beta(g) \frac{\partial}{\partial g} \right] (\chi' + \chi)(g, (q^2)^{1/2}/\mu) = 0, \quad (3.13)$$

the solution to which is

$$(\chi' + \chi)(g, (q^2)^{1/2}/\mu) = (\chi' + \chi)(\bar{g}((q^2)^{1/2}), 1), \quad (3.14)$$

where \bar{g} is the running coupling constant satisfying the equation

$$\frac{d\bar{g}(\mu')}{d\mu'} = \beta(\bar{g}(\mu')), \tag{3.15}$$

$$\bar{g}(\mu) = g.$$

Since QCD is asymptotically free, $\bar{g}^2(\mu')$ goes down as $C/\ln\mu'$ as $\mu' \rightarrow \infty$. Since $\chi' + \chi$ is proportional to \bar{g}^2 in lowest order in \bar{g} , it will go down as $1/\ln(q^2)^{1/2}$ as $(q^2)^{1/2} \rightarrow \infty$. The integral in the exponential of (3.12) then goes as

$$\int^{q^2} \frac{1}{\ln q'^2} d \ln q'^2 \sim \ln \ln q^2. \tag{3.16}$$

Just for ladder diagrams, however, there are no self-energy or vertex insertions, hence the effective β function is zero. Thus $\bar{g} = g$ and the term in the exponential goes as $\ln(Q/\mu)$.

IV. ANALYSIS OF GENERAL GRAPHS

A general graph contributing to the quark form factor in QCD cannot be directly treated by the method of Sec. III since they involve collinear divergences; i.e., these graphs receive contributions from the regions where one or more gluon lines are parallel to the outgoing quark or anti-quark line. Hence when the $\partial/\partial \ln p^+$ operator acts on an internal quark line it can give nonzero contribution if the quark line carries momentum from a gluon collinear to p . However, as we shall show, we may rearrange the graphs in such a way that none of the lines carry any momentum collinear to p except for self-energy insertion on external lines (a different rearrangement will bring them in a form where none of the momenta can be parallel to p). Then the operation of $\partial/\partial \ln p^+$ on such a graph may be treated in the same way as in Sec. III.

Thus the main task now is to show how to rearrange the graphs in the way mentioned above. To do this we use the Grammer-Yennie technique¹⁴ for factoring out the soft divergences. For factoring out soft divergences from lines collinear to p the Grammer-Yennie decomposition of a vertex ν of a gluon propagator $-iN^{\mu\nu}(k^2)/(k^2 + i\epsilon)$ is obtained as

$$N^{\mu\nu}(k) = N_{\tau}^{\mu}(k)[G^{\tau\nu}(k) + K^{\tau\nu}(k)], \tag{4.1}$$

where

$$G^{\tau\nu} = g^{\tau\nu} - \omega^{\tau}k^{\nu}/(\omega \cdot k + i\epsilon), \tag{4.2}$$

$$K^{\tau\nu} = \omega^{\tau}k^{\nu}/(\omega \cdot k + i\epsilon), \tag{4.3}$$

$$\omega = (1, 0, 0, 1),$$

and k is the momentum flowing from the ν vertex to the μ vertex. The G term has the property that if the momentum k is soft and if the ν end is

attached to a fermion or gluon line parallel to p , it gives a contribution which is suppressed by a power of q^2 (Ref. 14). The K term on the other hand gives us a simple answer if we sum over all possible insertions of the K gluon in a given Green's function. This is done with the help of Ward identities. The relevant Ward identities in the axial gauge are shown in Figs. 7(a) and 7(b). The arrow on the left-hand side of Fig. 7(a) represents a gluon, carrying polarization vector proportional to the gluon momentum k . a, b , and c are the group indices, while μ, ν, τ , and σ are the Lorentz indices. On the right-hand side, the circled vertices are proportional to $g^{\tau\nu}f^{abc}$ and $g^{\mu\sigma}f^{bac}$ for the first and the second figure, respectively. In Fig. 7(b) the arrow on the left-hand side again denotes a gluon with polarization vector proportional to k^{μ} . i, j are the group indices in quark representation while c is the group index in the gluon representation. Both the circled vertices on the right-hand side are proportional to $(T_c)_{ij}$. Some useful relations involving the circled vertices are shown in Figs. 7(c) and 7(d). These relations and the Ward identities may be derived by knowing the form of the QCD vertices and propagators in axial gauge. The precise expressions for the circled vertices are given in Appendix A.

We now give the algorithm for rearranging the graphs in a manner so that there cannot be any

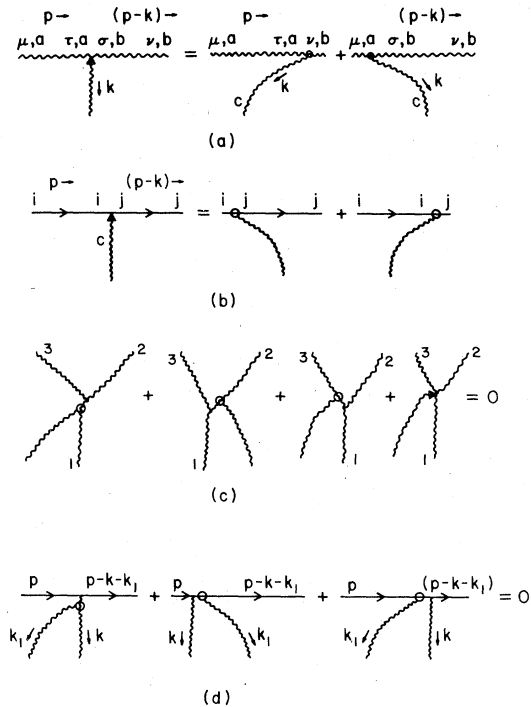


FIG. 7. Some useful Ward identities.

line collinear to p except in self-energy insertion on external lines. Let us start with a general graph of the form shown in Fig. 8. In all the following figures we shall denote the G vertex by a cross (this must be distinguished from the crossed fermion line of Sec. III).

Step I. We first identify the lines which can be collinear to p . In Fig. 8 all the gluons except S_0 , S_1 , S_2 , S_3 , and S_4 can be collinear to p . We also identify the gluons which are not potentially collinear to p but are attached to potentially collinear gluons. S_1 , S_2 , S_3 , and S_4 are such gluons in Fig. 8. Let us call the latter set N .

Step II. We identify the gluon which is a member of N and attached to the left-most point of the p' line (S_1 in Fig. 8) and locate the vertex where it is attached to a line potentially collinear to p . We decompose this end of the gluon (S_1) into the G and K parts and sum over all insertions of the K part on gluon lines and internal fermion loops which are potentially parallel to p , but we do not decompose (or sum over) the insertions of this gluon (S_1) on the outgoing quark line (defined in Sec. II). The result will be three types of graphs shown in Fig. 9. In any of these graphs we attribute a serial number of 1 to the S_1 gluon indicating that this is the first gluon to be decomposed into G and K gluons.

Step III. For graphs of type 9(b) or 9(c) we go to step V. For graphs of the type shown in Fig. 9(a), the presence of the G vertex reduces the number of gluons in the graph which can be parallel to p . For example the gluon lines S_5 , S_6 , and S_7 in Fig. 9(a) can no longer be collinear to p , because if S_1 is soft and S_5 and S_6 parallel to p then there is a suppression due to the G vertex on S_1 . One may wonder whether the presence of the G vertex may change some of the power-counting rules used in Ref. 13 but it is easy to check that it does not do so by investigating the behavior of the G vertex in different regions in momentum space.

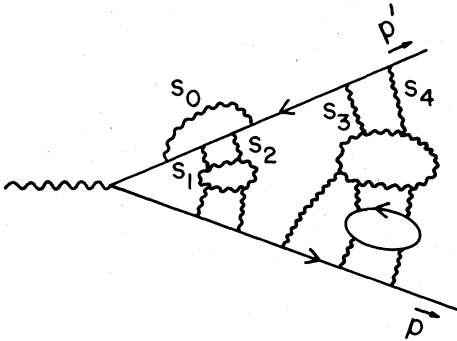


FIG. 8. A typical diagram contributing to the quark form factor.

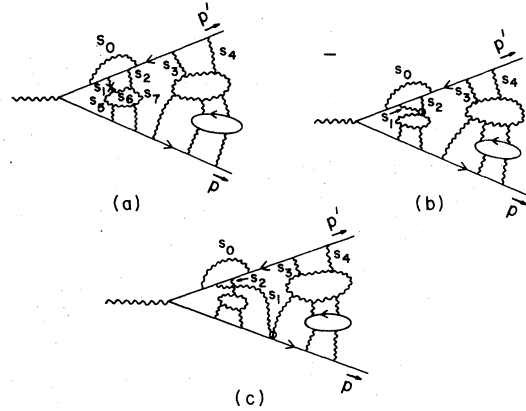


FIG. 9. Some typical diagrams obtained after completing step I of the algorithm for the diagram shown in Fig. 8.

We now identify the gluons which were potentially parallel to the p line before the S_1 gluon was decomposed but are no longer so and are attached to lines potentially parallel to p . S_5 and S_7 are such gluons in Fig. 9(a). We now keep all but one of these gluons fixed in position, decompose the remaining gluon into G and K gluons, and sum over all its insertions on gluon lines and fermion loops potentially parallel to p . Choosing S_5 in Fig. 9(a), the result will again be three types of diagrams shown in Fig. 10. [Diagrams 10(b) and 10(d) belong to the same type.] In all these graphs we attribute to the S_5 gluon the serial number 2 indicating that this is the second gluon which is being decomposed into G and K gluons. Next, in each of these graphs we break up the remaining gluons (S_7) one by one into G and K gluons and sum over all insertions of the S_7 gluon on gluon lines and fermion loops potentially parallel to p . However, if the line to which the S_7 gluon is attached ceases to be potentially parallel to p then we do not decompose the S_7 gluon [e.g., in Fig. 10(a)]. Also if S_7 has any other gluon attached to it through a circled vertex [as S_5 in Fig. 10(b)], then in the Grammer-Yennie decomposition of the vertex we use the combined momentum of S_5 and S_7 for k in Eq. (4.2). This allows us to apply the Ward identity in its usual form for the K vertex. In order to preserve the symmetry between the S_5 and the S_7 gluons we consider another series of graphs where the S_7 gluon is decomposed into G and K gluons before the S_5 gluon, and we sum over all insertions of the S_7 gluon first; then we decompose the S_5 gluon. This calls for a factor of $1/2!$ multiplying each graph since we are counting each graph twice. (In the general case we have a factor of $1/n!$ where n is the number of soft gluons to be decomposed.)

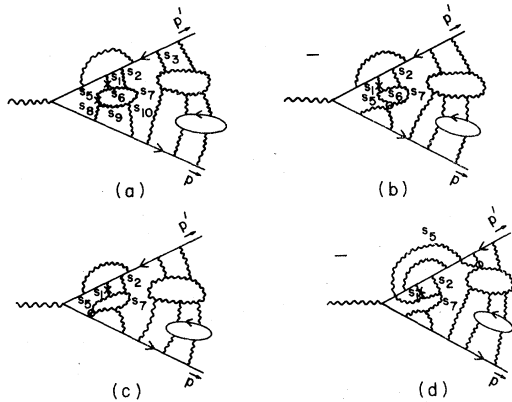


FIG. 10. Typical diagrams obtained after decomposing the S_5 gluon into G and K gluon and summing over all insertions of the K part on gluon lines and fermion loops potentially parallel to p in Fig. 9(a).

Step IV. We consider every graph obtained after the completion of step III and identify the gluons prevented from being parallel to p due to the Grammer-Yennie decomposition of S_5 and S_7 gluons. S_8 , S_9 , and S_{10} are such lines in Fig. 10(a). We repeat the procedure given in step III with these gluons. This process is continued until we can prevent as many gluon lines and fermion loops as possible from being potentially parallel to p . For example, in Fig. 10(a) we cannot decompose S_8 or S_{10} gluons (remember that G - K decomposition is forbidden when the gluon lines are attached to the outgoing quark line). Thus we stop here and to step V. Figure 11 is another example where we should move to step V.

Step V. This step deals with diagrams of the type shown in Figs. 9(b) and 9(c) obtained after step I and also diagrams of the type shown in Figs. 10(a) and 11 obtained after step IV. We take the next member of the set N (S_2) attached to the next

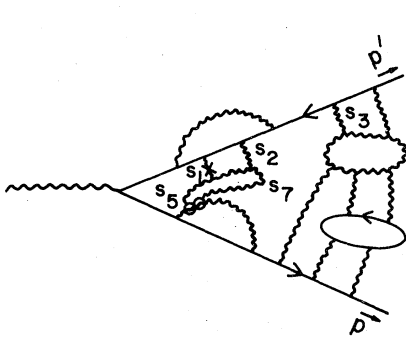


FIG. 11. A typical diagram obtained from Fig. 10(c) after summing over all insertions of the K part of the S_7 gluon on gluon lines and fermion loops which are potentially parallel to p .

innermost point of the p' line and check whether it is attached to a gluon line or fermion loop potentially parallel to p . If it is, then we decompose this into G and K gluons and repeat steps II, III, and IV with this gluon. Otherwise we move to the next innermost gluon of set N attached to the p' line. In Figs. 9(b) and 9(c), S_2 is indeed attached to a line potentially parallel to p . However, in Figs. 10(a) and 11 it is not; hence we must move to the S_3 gluon for the latter figures. This process is continued until we exhaust all the gluons of set N .

Some typical graphs obtained at the end of step V have been shown in Fig. 12. Note that in any of these graphs a gluon line not potentially parallel to p may meet a gluon line potentially parallel to p only through a circled vertex at the point where the latter meets the outgoing quark line. For example, let us take the diagram shown in Fig. 12(a). The gluon S_1 cannot be parallel to p since it is attached to the p' line; however, it may either be parallel to p' or be contracted or be soft. In the first two cases the line S_5 cannot be parallel to p by power counting, while in the third case if S_5 is parallel to p , we shall have a soft gluon attached to a line parallel to p through a G vertex and this contribution is also suppressed. Using this type of argument we can analyze the other parts of the graph also and see that the only line in this graph potentially parallel to p is the S_{10} gluon shown in the figure in thick lines. In all the graphs in this figure the gluon lines and fermion loops potentially parallel to p are shown by thick lines.

There is one possible place where the type of argument given above may break down, namely, when the G vertex is a part of a contracted three-point vertex. Consider the diagram shown in Fig. 13, which is a possible subdiagram of a graph after we complete step V of our algorithm. Suppose the

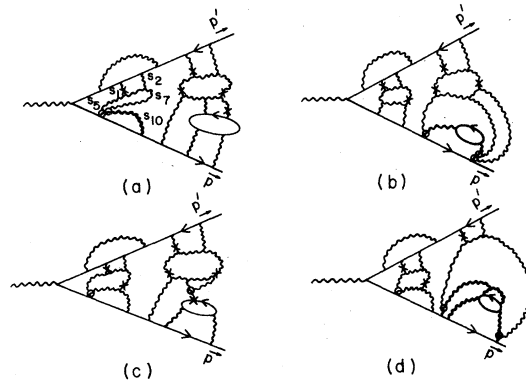


FIG. 12. Typical diagrams obtained after completion of step V of the algorithm.

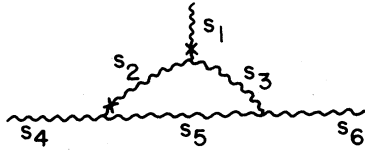


FIG. 13. A potentially dangerous subdiagram.

gluon S_1 is soft. Then by the previous argument S_2 and S_3 are constrained not to be parallel to p . If S_2 is soft then again by the same argument S_4 , S_5 , and S_6 are constrained not to be parallel to p . However, if S_2 , S_3 , and S_5 are contracted then S_4 and S_6 may be parallel to p since attachment of soft lines to jet lines through contracted three-point vertices is not suppressed by power counting. In Appendix B we show how such contributions are suppressed.

Step VI. Now decompose the gluons, which are not potentially parallel to p and are attached to the outgoing quark line, into G and K gluons and sum over all insertions. During this process we follow the same serial order of decomposition as was followed during the decomposition of the gluons attached to gluon lines and fermion loops potentially parallel to p . For example, in Fig. 12(a) the gluon S_5 is decomposed before the gluon S_7 . Hence with this we first add the diagrams where the S_5 gluon is attached to the outgoing quark line, decomposed into G and K gluons and summed over all K -gluon insertions. The diagram of Fig. 12(a) will then cancel the diagrams shown in Fig. 14. In the diagrams with G vertices on the outgoing quark line, a certain subset of lines including the part of the quark line to the left of the G vertex are constrained to be contracted, these lines being separated from the rest of the diagram by a two-particle $q\bar{q}$ intermediate state. For example, in Fig. 15 all lines inside the dashed box are constrained to be contracted. Again there is an apparent problem if the G vertex is a part of a contracted three-point vertex, and this is taken care of in Appendix B.

During the decomposition, whenever we run into a G vertex on the outgoing quark line we identify the

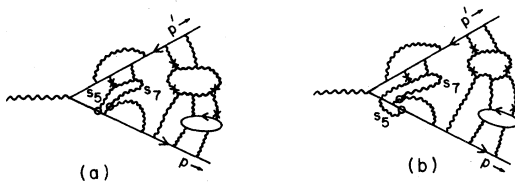


FIG. 14. Diagrams that cancel Fig. 12(a).

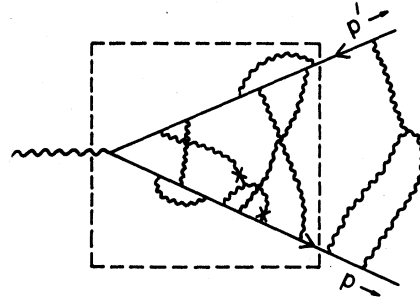


FIG. 15. A typical diagram obtained when we start decomposing the gluons attached to the outgoing quark line into G and K gluons.

part of the diagram constrained to be contracted by the presence of this vertex and do not further decompose any of the lines inside this blob. For the lines outside the contracted blob we carry on the decomposition procedure in the usual way. As a result, at the end of the decomposition procedure all the gluon lines, potentially parallel to p , are completely decoupled from the rest of the diagram and we obtain diagrams whose sum may be represented in the abstract form shown in Fig. 16 (ignoring terms which do not have poles in p). Here Γ_{UV} includes diagrams all lines of which are constrained to be contracted due to the presence of G vertices on the outgoing quark line. Typical contributions to Γ_{UV} have been shown in Fig. 17. The blob E is one-particle irreducible (1PI) in the external \bar{q} line and contains internal gluon lines fermion loops all of which are constrained to be non-parallel to p due to the presence of G vertices. The crossed circled vertex on the p line contains various combinations of circled vertices. Typical contributions involving E have been shown in Fig. 18. Note that in order to draw diagrams which contribute to E or Γ_{UV} we must obey the rules which govern the order in which different gluons are decomposed. Figure 19 shows an example of a diagram that is not present in Γ_{UV} ; Fig. 20 shows an example of a diagram that is not present in E —although at the first sight they seem to be

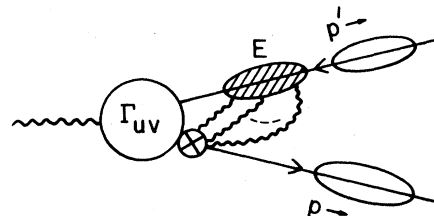


FIG. 16. Rearranged form of the form factor after completion of step VI of the algorithm.

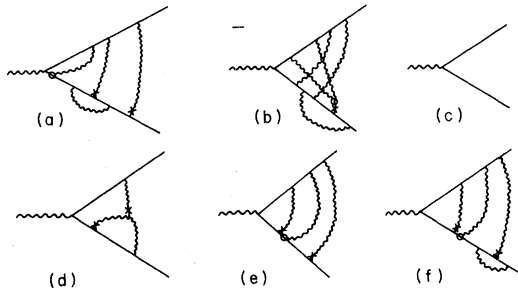


FIG. 17. Typical contributions to Γ_{UV} .

so. Figure 19 may be obtained only if the gluon S_2 is decomposed before S_1 ; however, our rule for decomposition says that S_1 always has to be decomposed before S_2 since it is attached to the innermost point of the p' line. The same is the case with Fig. 20. Also our decomposition rule avoids diagrams like the one shown in Fig. 21. Note that this diagram cannot be brought into the form shown in Fig. 16 since in this the gluon S_2 may be soft al-

$$\bar{u}(p)(\not{p}-m) \frac{1}{[Z_2(p)]^{1/2}} \frac{Z_2(p)}{\not{p}-m} \Gamma(p,p') \frac{Z_2(p')}{\not{p}'-m} \frac{1}{[Z_2(p')]^{1/2}} (\not{p}'-m)v(p') = \bar{u}(p)[Z_2(p)]^{1/2} \Gamma(p,p')[Z_2(p')]^{1/2} v(p'). \tag{4.4}$$

$\Gamma(p,p')$ is diagrammatically represented as in Fig. 22. Thus we have achieved the goal of decoupling the potentially parallel to p lines from the rest of the diagram. We now study the behavior of $\Gamma(p,p')$. The behavior of $Z_2(p)$ will be analyzed in the next section. Note that the form of $\Gamma(p,p')$ given in Fig. 22 is not suitable for applying the technique of Sec. III. To tackle this problem we use a trick developed by Collins and Sterman¹² which involves the observation that if we consider the contribution to the form factor obtained after step V of our algorithm (typical members of which are shown in Fig. 12), keep only those diagrams which do not have gluon lines potentially parallel to p [e.g., Fig. 12(c)], and decompose and sum over the gluons attached to the outgoing quark line according to the algorithm of step VI, then the K -gluon part will give a contribution which exactly

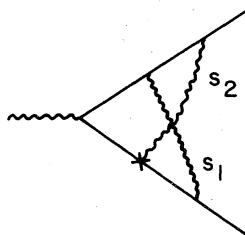


FIG. 19. A diagram which is not present in Γ_{UV} .

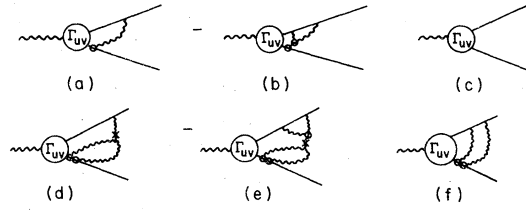


FIG. 18. Typical contributions coming from E .

though S_1 is contracted, because if k be the momentum carried by the S_2 gluon then in the limit $k/(q^2)^{1/2} \rightarrow 0$ we get four powers of k in the denominator [two powers from the S_2 propagator, one power from the circled vertex ($\propto 1/k^2$), and one power from the outer part of the p' line]. The white blobs on the external lines in Fig. 16 represent full self-energy insertions on external lines. Hence if we call the combined contribution of E and Γ_{UV} to be Γ , the Sudakov form factor may be written as

looks like the E part of Fig. 22. To formulate this more precisely let us first define a vertex function $\Gamma_{UV}^0(k)$ which is constructed by summing over a subset of diagrams contributing to $\Gamma_{UV}(k)$ (the argument k denotes that the momentum of the outgoing quark line is $p+k$ and that of the outgoing antiquark line is $p'-k$). In constructing Γ_{UV}^0 we exclude those diagrams from Γ_{UV} in which if in the outermost two-particle-irreducible part we replace all the G vertices on the quark line by ordinary vertices we do not get any gluon line potentially parallel to p [e.g., Figs. 17(a), 17(d), and 17(e)]. This is done to avoid double counting as we see below. Γ_{UV}^0 includes the bare vertex proportional to $\epsilon \cdot \gamma$ [Fig. 17(c)]. We define $F^0(k,k')$ to be the sum of $q\bar{q} \rightarrow q\bar{q}$ graphs with the incoming particles carrying momenta $p+k$ and $p'-k'$, respectively. The internal vertices of F^0 however are

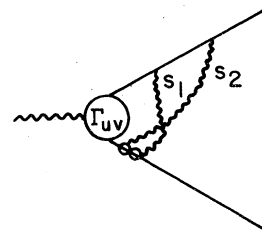


FIG. 20. A diagram which is not present in E .

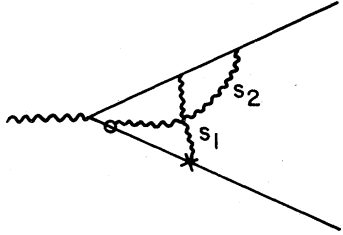


FIG. 21. A diagram which is not present in the rearranged form of the form factor after completion of step VI of the algorithm.

not the ordinary vertices. Rather we construct F^0 by starting with an ordinary $q\bar{q} \rightarrow q\bar{q}$ graph, following the decomposition procedure of steps I to V of our algorithm, and ignoring all diagrams obtained at the end of step V which contain gluon lines potentially parallel to p . Also as a convention we include the self-energy insertions on the incoming antiquark line ($p' - k'$) but truncate the propagator of the outgoing antiquark line. Note that by definition of F^0 self-energy insertions on quark lines are eliminated since they include lines potentially parallel to p . We include the propagator $i/(\not{p} - \not{k} - m_R)$ of the incoming quark line in F^0 but not the propagator $i/(\not{p} - \not{k}' - m_R)$ of the outgoing quark line. Typical contributions to F^0 have been shown in Fig. 23. Note that F^0 also includes the trivial term $(2\pi)^4 \delta^4(k - k')$ [Fig. 23(a)].

Let us now consider the amplitude

$$\int \Gamma_{UV}^0(k) F^0(k, 0) d^4k / (2\pi)^4, \quad (4.5)$$

which can be diagrammatically represented as in Fig. 24. If we now reduce this diagram using step VI of our algorithm and if for the time being we ignore the terms with circled vertices attached to the extreme right end of the quark line we shall get back Fig. 22. This is because the E part that we shall get from Fig. 24 does not depend on whether there are gluon lines, potentially collinear to p , present in the diagram or not (the latter be-

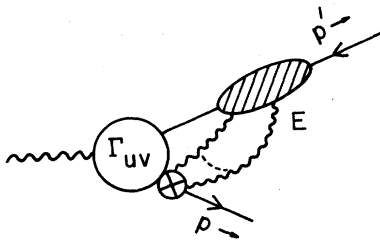


FIG. 22. Graphical representation of $\Gamma(p, p')$.

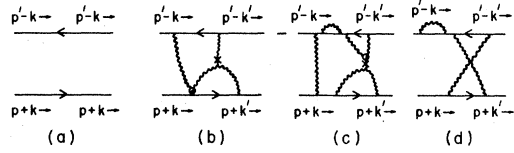


FIG. 23. Typical contributions to $F^0(k, k')$.

ing always decoupled from the rest of the diagram after completion of step VI of the algorithm). Also terms in Γ_{UV} that are missing in Γ_{UV}^0 are obtained back when we consider the contribution to Fig. 24 with some of the gluons in F^0 attached to the outgoing quark line through a G vertex. This is why those terms were left out in the definition of Γ_{UV}^0 . However, this time we also have diagrams where some gluons are attached to the extreme right end of a quark line through circled vertices (e.g., graphs shown in Fig. 25). They are proportional to $\not{p} - m_R$ which when multiplied by $u(p)$ gives $m - m_R$. But since in our renormalization scheme we choose m_R to be equal to m such terms vanish. Expression (4.5) is then equal to $\Gamma(p, p')$. Any other choice of m_R will unnecessarily complicate the proof.

Let us define $K^0(k, k')$ to be the sum of all two-particle-irreducible $q\bar{q} \rightarrow q\bar{q}$ graphs constructed using the same rules as $F^0(k, k')$. Again by convention we include the propagator of the incoming lines in K^0 but not those of the outgoing lines. In this sense K^0 is not strictly two-particle irreducible. Typical contributions to K^0 are shown in Fig. 26. We now follow the trick of Sec. III to write expression (4.5) as

$$\Gamma(p, p') = \int \lambda_0 \epsilon \cdot \gamma F^0(k, 0) d^4k / (2\pi)^4 + \int [\Gamma_{UV}^0(k) - \lambda_0 \epsilon \cdot \gamma] F^0(k, 0) d^4k / (2\pi)^4, \quad (4.6)$$

where $\lambda_0 \epsilon \cdot \gamma$ is the part of $\Gamma_{UV}^0(k)$ which contributes in the limit $|k^\mu| \ll (q^2)^{1/2}$ [just as $\lambda_0 \epsilon \cdot \gamma$ was an approximation for $\phi(k)$ for $|k^\mu| \ll (q^2)^{1/2}$ in Sec. III]. Now F^0 satisfies the integral equation

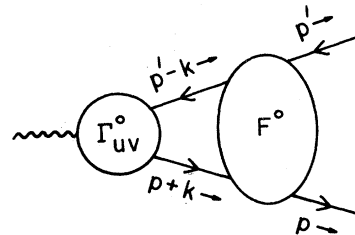


FIG. 24. Graphical representation of Eq. (4.5).

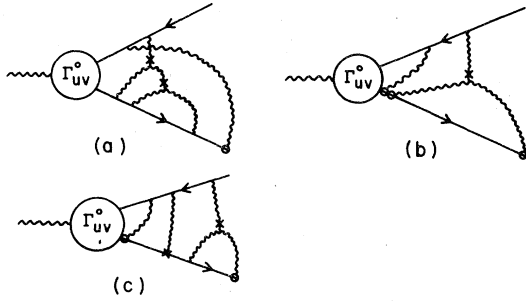


FIG. 25. Typical diagrams with circled vertices on the rightmost end of the quark line, obtained after the decomposition of Fig. 24.

$$F^0(k, k') = (2\pi)^4 \delta^4(k - k') + \int K^0(k, k'') F^0(k'', k') d^4 k'' / (2\pi)^4. \quad (4.7)$$

With the help of this equation we may proceed as in Sec. III and get

$$\Gamma(p, p') = (\lambda_0 + \lambda_1 + \lambda_2 + \dots) \int \epsilon \cdot \gamma F^0(k, 0) d^4 k / (2\pi)^4, \quad (4.8)$$

λ 's being functions of $(q^2)^{1/2}$, μ , and g only.

Now we let the derivative operator $\partial/\partial \ln p^+$ act on Γ . Since Γ does not have any line potentially collinear to p we can carry out the analysis of Sec. III and show that

$$\frac{\partial \Gamma}{\partial \ln p^+} = (\psi_0 + \psi_1 + \psi_2 + \dots) \int \epsilon \cdot \gamma F^0(k, 0) d^4 k / (2\pi)^4, \quad (4.9)$$

where ψ_0, ψ_1, \dots are functions of $(q^2)^{1/2}$, μ , and g only. Thus,

$$\frac{\partial \Gamma}{\partial \ln p^+} = \chi \Gamma, \quad (4.10)$$

where

$$\chi = (\psi_0 + \psi_1 + \dots) / (\lambda_0 + \lambda_1 + \dots). \quad (4.11)$$

Note that although Γ may contain lines potentially collinear to p' , χ contains only contracted lines. In a similar manner we can decompose the form factor in such a way that all lines potentially parallel to p' go into the self-energy part and hence show that

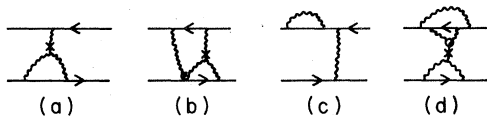


FIG. 26. Typical contributions to K^0 .

$$\frac{\partial \Gamma}{\partial \ln p'^-} = \chi' \Gamma. \quad (4.12)$$

Thus,

$$\frac{\partial \Gamma}{\partial \ln (q^2)^{1/2}} = \frac{\partial \Gamma}{\partial \ln p^+} + \frac{\partial \Gamma}{\partial \ln p'^-} = (\chi + \chi') \Gamma, \quad (4.13)$$

the solution to which is

$$\Gamma = A(\mu, m, \tau, g) \times \exp \left[\int^{(q^2)^{1/2}} (\chi + \chi')(\mu, (q'^2)^{1/2}, g) \times d(q'^2)^{1/2} / (q'^2)^{1/2} \right], \quad (4.14)$$

A being an unknown function. For QCD $\chi + \chi'$ goes as $1/\ln(q'^2)^{1/2}$. Hence the term in the exponential is

$$\int^{(q^2)^{1/2}} (\chi + \chi')(\mu, (q'^2)^{1/2}, g) d(q'^2)^{1/2} / (q'^2)^{1/2} \sim \ln \ln (q^2)^{1/2}. \quad (4.15)$$

Note that one of the crucial conditions to be satisfied by $K^0(k, k')$ is that if the incoming momentum k is constrained to be of order $(q^2)^{1/2}$ in all components, all the lines inside K^0 must also be constrained to carry momentum $\sim (q^2)^{1/2}$ by power counting, otherwise the λ 's and the ψ 's will contain infrared logarithms. The fact that this is true is apparent from the rules of construction of K^0 .

Figure 27 shows an example of a diagram which, if included in K^0 , would not have satisfied this condition, since even if the momentum k is of order $(q^2)^{1/2}$, the gluon line S_2 may carry soft momentum if k' is small. This is because the propagator of S_2 carries two powers of its momentum in the denominator, the circled vertex carries one power of k_2 in the denominator, and the line $p' - k' + k_2$ carries one more. Thus the integral over k_2 may give logarithms of $(q^2)^{1/2} / |k'|^\mu$. However, this is not an allowed diagram in K^0 , because this will appear only if S_2 is decomposed before S_1 ; however, since S_1 is attached to the left of S_2 on the antiquark line it has to be decomposed first.

Also note that if the $\partial/\partial \ln p^+$ operator acts on a part of the fermion line, which is a part of an internal composite three-point gluon-fermion vertex

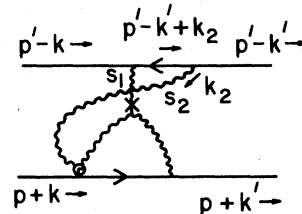


FIG. 27. A contribution not to be included in K^0 .

(as shown in Fig. 28), then we may get a contribution from a region in momentum space where all the lines inside this composite vertex are contracted but the gluon (S) attached to this composite vertex is still soft. If such regions are really present they would upset our analysis; however, we have shown in Appendix B that contributions from such regions are suppressed.

V. ANALYSIS OF $Z_2(p)$ USING THE CONSTRAINT OF LORENTZ INVARIANCE OF THE FORM FACTOR

Equation (4.4) gives the expression for the Sudakov form factor. We have found the asymptotic behavior of $\Gamma(p, p')$ in the last section. In order to find the full Sudakov form factor we must evaluate the functions $Z_2(p)$ and $Z_2(p')$. In this section we shall show that the constraint of Lorentz invariance for expression (4.4) is sufficient to give us the form of the functions $Z_2(p)$ and $Z_2(p')$. Such techniques have been used in the past by Frenkel and Taylor¹⁶ and by Mason.¹⁷

To see this let us note that $Z_2^{1/2}(p)$ and $Z_2^{1/2}(p')$ are pure numbers in the limit $p^+ \rightarrow \infty$ and $p'^- \rightarrow \infty$,

respectively, as shown in Appendix B. Also the part of $\Gamma(p, p')$ which contributes to the amplitude in leading power in q^2 must be proportional to $\epsilon \cdot \gamma$; let us call this $V(p, p')\epsilon \cdot \gamma$. Then the quantity

$$Z_2^{1/2}(p)V(p, p')Z_2^{1/2}(p') \quad (5.1)$$

must be a function of $p \cdot p'$ only but not of $n \cdot p$ and $p' \cdot n$ if we want to satisfy the condition of Lorentz invariance of the final amplitude. Let us call it $F(p \cdot p')$. Now in the kinematic configuration described in Sec. II, p and p' are completely specified if we specify p^+ and p'^- , respectively. Hence we may write

$$Z_2^{1/2}(p^+, g)V(p^+, p'^-, g)Z_2^{1/2}(p'^-, g) = F(p^+ p'^-, g). \quad (5.2)$$

Here we have explicitly exhibited the dependence of the functions on the coupling constant g and p^+ and p'^- but suppressed their dependence on m , μ , and τ . It should be kept in mind that all the functions that appear in the discussion from now on are functions of m , μ , and τ unless otherwise stated. Differentiating both sides of Eq. (5.2) with respect to p^+ , we get

$$\frac{\partial Z_2^{1/2}(p^+, g)}{\partial p^+} V(p^+, p'^-, g)Z_2^{1/2}(p'^-, g) + Z_2^{1/2}(p^+, g) \frac{\partial V(p^+, p'^-, g)}{\partial p^+} Z_2^{1/2}(p'^-, g) = p'^- F'(p^+ p'^-, g), \quad (5.3)$$

where

$$F'(\chi, g) = \frac{\partial F(\chi, g)}{\partial \chi}. \quad (5.4)$$

Similarly, differentiating Eq. (5.2) with respect to p'^- we get

$$Z_2^{1/2}(p^+, g)V(p^+, p'^-, g) \frac{\partial Z_2^{1/2}(p'^-, g)}{\partial p'^-} + Z_2^{1/2}(p^+, g) \frac{\partial V(p^+, p'^-, g)}{\partial p'^-} Z_2^{1/2}(p'^-, g) = p^+ F'(p^+ p'^-, g). \quad (5.5)$$

Eliminating F' from (5.3) and (5.5) we get

$$Z_2^{-1/2}(p^+, g)p^+ \frac{\partial Z_2^{1/2}(p^+, g)}{\partial p^+} + V^{-1}(p^+, p'^-, g)p^+ \frac{\partial V(p^+, p'^-, g)}{\partial p^+} = Z_2^{-1/2}(p'^-, g)p'^- \frac{\partial Z_2^{1/2}(p'^-, g)}{\partial p'^-} + V^{-1}(p^+, p'^-, g)p'^- \frac{\partial V(p^+, p'^-, g)}{\partial p'^-}. \quad (5.6)$$

Now $V^{-1}p^+(\partial V/\partial p^+)$ and $V^{-1}p'^-(\partial V/\partial p'^-)$ are nothing but the functions χ and χ' defined in Eqs. (4.10) and (4.12), respectively. As found in Sec. IV, the functions χ and χ' are free of ultraviolet divergences and also independent of m and the infrared regulator τ . Hence they satisfy the renormalization-group equation.

$$\left(\mu \frac{\partial}{\partial \mu} + \beta(g) \frac{\partial}{\partial g}\right) \chi(p^+, p'^-, g, \mu) = 0, \quad (5.7)$$

$$\left(\mu \frac{\partial}{\partial \mu} + \beta(g) \frac{\partial}{\partial g}\right) \chi'(p^+, p'^-, g, \mu) = 0.$$

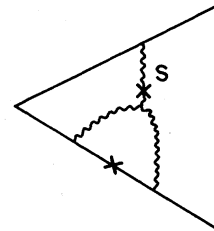


FIG. 28. A potentially dangerous diagram by naive power counting.

Here we have explicitly exhibited the dependence of χ and χ' on μ . Also note that, unlike in the previous sections, here we are treating p^+ and p'^- as independent variables; hence χ and χ' are regarded as functions of p^+ as well as p'^- instead of a single variable q^2 .

Solutions of (5.7) are

$$\begin{aligned}\chi(p^+, p'^-, g, \mu) &= \chi(p^+/\lambda, p'^-/\lambda, \bar{g}(\mu\lambda), \mu), \\ \chi'(p^+, p'^-, g, \mu) &= \chi'(p^+/\lambda, p'^-/\lambda, \bar{g}(\mu\lambda), \mu),\end{aligned}\quad (5.8)$$

where λ is an arbitrary number. Let us define

$$\begin{aligned}A(p^+, g) &= Z_2^{-1/2}(p^+, g) p^+ \frac{\partial Z_2^{1/2}(p^+, g)}{\partial p^+}, \\ B(p'^-, g) &= Z_2^{-1/2}(p'^-, g) p'^- \frac{\partial Z_2^{1/2}(p'^-, g)}{\partial p'^-}.\end{aligned}\quad (5.9)$$

Equation (5.6) may then be written as

$$A(p^+, g) - B(p'^-, g) = \chi''(p^+, p'^-, g, \mu), \quad (5.10)$$

where

$$\begin{aligned}\chi''(p^+, p'^-, g, \mu) &= \chi'(p^+, p'^-, g, \mu) \\ &\quad - \chi(p^+, p'^-, g, \mu).\end{aligned}\quad (5.11)$$

Using Eqs. (5.8), (5.10), and (5.11) we get

$$\begin{aligned}A(p^+, g) - B(p'^-, g) &= A(p^+/\lambda, \bar{g}(\lambda\mu)) \\ &\quad - B(p'^-/\lambda, \bar{g}(\lambda\mu))\end{aligned}\quad (5.12)$$

or

$$A(p^+, g) - A(p^+/\lambda, \bar{g}(\lambda\mu)) = B(p'^-, g) - B(p'^-/\lambda, \bar{g}(\lambda\mu)). \quad (5.13)$$

Now the left-hand side of the above equation is a function of p^+ , λ , and g while the right-hand side is a function of p'^- , λ , and g (of course both sides are also functions of m , τ , and μ). Thus in order that Eq. (5.13) is satisfied for arbitrary values of p^+ and p'^- , both sides of the equation must be independent of p^+ as well as p'^- . Let us denote this by $C(\lambda, g)$. Equation (5.13) then gives

$$\begin{aligned}A(p^+, g) - A(p^+/\lambda, \bar{g}(\lambda\mu)) &= C(\lambda, g), \\ B(p'^-, g) - B(p'^-/\lambda, \bar{g}(\lambda\mu)) &= C(\lambda, g).\end{aligned}\quad (5.14)$$

Let us take $\lambda = 1 + \epsilon$. Equations (5.14) show that $C(1, g) = 0$ since the left-hand side vanishes at $\lambda = 1$. Thus if we define

$$C_1(g) = \left. \frac{\partial C(\lambda, g)}{\partial \lambda} \right|_{\lambda=1}, \quad (5.15)$$

Eq. (5.14) in the limit $\epsilon \rightarrow 0$ becomes

$$A(p^+, g) - A(p^+ - \epsilon p^+, \bar{g}(\mu + \epsilon\mu)) = \epsilon C_1(g) \quad (5.16)$$

and a similar equation for B . Then, using Eq. (3.15) we get

$$p^+ \frac{\partial A(p^+, g)}{\partial p^+} - \beta(g) \frac{\partial A(p^+, g)}{\partial g} = C_1(g), \quad (5.17)$$

$$p'^- \frac{\partial B(p'^-, g)}{\partial p'^-} - \beta(g) \frac{\partial B(p'^-, g)}{\partial g} = C_1(g).$$

The solutions to Eqs. (5.17) are,

$$A(p^+, g) = A(\mu, \bar{g}(p^+)) + \int_{\mu}^{p^+} C_1(\bar{g}(x)) \frac{dx}{x}, \quad (5.18)$$

$$B(p'^-, g) = B(\mu, \bar{g}(p'^-)) + \int_{\mu}^{p'^-} C_1(\bar{g}(x)) \frac{dx}{x}.$$

Using Eqs. (5.9) and (5.18), we get

$$\begin{aligned}Z_2^{1/2}(p, g) &= \exp \left\{ \int_{\mu}^{p^+} \frac{dx'}{x'} \left[\int_{\mu}^{x'} C_1(\bar{g}(x)) \frac{dx}{x} \right. \right. \\ &\quad \left. \left. + A(\mu, \bar{g}(x)) \right] \right\} Z_2^{1/2}(\mu, g),\end{aligned}\quad (5.19)$$

$$\begin{aligned}Z_2^{1/2}(p', g) &= \exp \left\{ \int_{\mu}^{p'^-} \frac{dx'}{x'} \left[\int_{\mu}^{x'} C_1(\bar{g}(x)) \frac{dx}{x} \right. \right. \\ &\quad \left. \left. + B(\mu, \bar{g}(x)) \right] \right\} Z_2^{1/2}(\mu, g)\end{aligned}\quad (5.20)$$

where

$$\begin{aligned}Z_{2^+}^{1/2}(\mu, g) &= Z_2^{1/2}(p^+ = \mu, g), \\ Z_{2^-}^{1/2}(\mu, g) &= Z_2^{1/2}(p'^- = \mu, g).\end{aligned}\quad (5.21)$$

Note that Eqs. (5.17) are valid only for p^+ , $p'^- \gg m$, hence the solutions (5.18) are not exact if we choose $\mu \sim m$, since these assume the differential Eqs. (5.17) to be valid even for $p^+ \sim \mu$. This problem may be remedied by taking μ/m to be a large but fixed number so that we can ignore terms of order m/μ and then the Eqs. (5.17) are valid up to order (m/μ) . The same remark holds for the quantities $Z_{2^+}^{1/2}(\mu, g)$ and $Z_{2^-}^{1/2}(\mu, g)$.

Also note that the constants $A(\mu, \bar{g}(x))$, $B(\mu, \bar{g}(x))$, $Z_{2^+}^{1/2}(\mu, g)$, $Z_{2^-}^{1/2}(\mu, g)$, and $C_1(g)$ are in general functions of μ , m , and τ and may also diverge in the limit $\tau \rightarrow 0$. Equations (5.19) and (5.20) give the behavior of $Z_2^{1/2}(p^+, g)$ and $Z_2^{1/2}(p'^-, g)$ as functions of p^+ and p'^- , respectively, at fixed m , μ , and τ . In lowest-order perturbation theory $C_1(g)$ goes as g^2 [as can be seen from Eqs. (5.17)]. Thus using asymptotic freedom of QCD we may write

$$C_1(\bar{g}(x)) \sim 1/\ln x \quad \text{as } x \rightarrow \infty, \quad (5.22)$$

$$\int_{\mu}^{x'} \frac{dx''}{x''} \int_{\mu}^{x'} C_1(\bar{g}(x)) \frac{dx}{x} \sim \ln(p^+/\mu) (\ln \ln p^+/\mu). \quad (5.23)$$

Thus we see that the leading term in the exponential for $Z_2^{1/2}(p)$ goes as $\ln \ln(p^+/\mu) \times \ln(p^+/\mu)$. The coefficient of this term may be calculated either by

evaluating $C_1(g)$ in lowest-order perturbation theory or by comparing the result with one-loop calculation of form factor. This will be illustrated in Sec. VI. But here we can make the comment that the coefficient of this leading term in the exponential will be independent of m and τ . This is because χ'' in Eq. (5.10) is independent of m and τ ; hence any m and τ dependence of A and B must be of the form of an additive constant independent of p^+ and p' . This implies that the coefficients of the leading term $(\ln p^+)(\ln \ln p^+)$ in $Z_2^{1/2}(p)$ and $(\ln p'^-)(\ln \ln p'^-)$ in $Z_2^{1/2}(p')$ are independent of m and τ .

VI. A MORE DIRECT EVALUATION OF $Z_2(p)$

In this section we give a method for more direct evaluation of $Z_2(p)$. The renormalized quark propagator in the axial gauge goes as

$$S_F(p) = [Z_2(p)]^{1/2} \frac{i}{\not{p} - m} [\bar{Z}_2(p)]^{1/2} \quad (6.1)$$

near the mass shell. Here $[Z_2(p)]^{1/2}$ and $[\bar{Z}_2(p)]^{1/2}$ are finite wave-function renormalization factors which are in general γ matrix functions of μ , m_R , τ , p , and n . They are related to each other by

$$[\bar{Z}_2(p)]^{1/2} = \gamma^0 [Z_2(p)^\dagger]^{1/2} \gamma^0. \quad (6.2)$$

As shown in Appendix B, in the limit $|\vec{p}| \rightarrow \infty$, $[Z_2(p)]^{1/2}$ reduces to an identity matrix in Dirac space; i.e., it is a simple c -number function of p , n , μ , m_R , and τ .

We shall study the change of $S_F(p)$ under an infinitesimal boost β along the z axis which changes a four-vector k to k' by

$$\begin{aligned} k'^+ &= \gamma k^+ (1 + \beta), \\ k'^- &= \gamma k^- (1 - \beta), \\ k'^i &= k^i \quad (i=1, 2). \end{aligned} \quad (6.3)$$

Let us write these transformations as

$$\begin{aligned} k'^\mu &= \Lambda^\mu_\nu k^\nu, \\ k'_\mu &= \Lambda_\mu^\nu k_\nu. \end{aligned} \quad (6.4)$$

Also we shall define $p' = \Lambda p$ and the reader should not confuse this with the momentum of the outgoing antiquark. Let S be the Lorentz-transformation operator in Dirac space corresponding to the above boost such that

$$S k \cdot \gamma S^{-1} = k' \cdot \gamma. \quad (6.5)$$

Then, near $p^2 = p'^2 = m^2$,

$$S_F(p') - S S_F(p) S^{-1} = \{ [Z_2(p')]^{1/2} - [Z_2(p)]^{1/2} \} \frac{i}{\not{p}' - m} [\bar{Z}_2(p)]^{1/2} + [Z_2(p')]^{1/2} \frac{i}{\not{p}' - m} \{ [\bar{Z}_2(p')]^{1/2} - [\bar{Z}_2(p)]^{1/2} \}. \quad (6.6)$$

Although $[Z_2(p')]^{1/2} = [\bar{Z}_2(p')]^{1/2}$, we prefer to distinguish between the two for reasons which will become clear soon. Now the contribution to $S_F(p)$ from Feynman diagrams may be written as

$$S_F(p) = \sum_F \int \left[\prod_{i=1}^r \frac{d^4 l_i}{(2\pi)^4} \right] F_{\mu_1, \dots, \mu_n \nu_1, \dots, \nu_n}^{a_1, \dots, a_n b_1, \dots, b_n}(p, l_i) \prod_{j=1}^n N_{a_j b_j}^{\mu_j \nu_j}(q_j), \quad (6.7)$$

where \sum_F denotes the sum over all Feynman diagrams, l_1, \dots, l_n are the r independent loop momenta, $F_{\mu_1, \dots, \mu_n \nu_1, \dots, \nu_n}^{a_1, \dots, a_n b_1, \dots, b_n}(p, l_i)$ is a Lorentz-covariant γ matrix function of the external momentum p , and the independent loop momenta l_i , which includes contributions from fermion propagators and all the vertices and $N^{\mu_j \nu_j}(q_j)$, $j=1, \dots, n$ are the gluon propagators of n internal gluons present in the diagram. The q_i 's are thus linear combinations of the loop momenta.

Using the Lorentz covariance of F and Lorentz invariance of $d^4 l_i$, we may write

$$S S_F(p) S^{-1} = \sum_F \int \left[\prod_{i=1}^r \frac{d^4 l'_i}{(2\pi)^4} \right] F_{\mu_1, \dots, \mu_n \nu_1, \dots, \nu_n}^{a_1, \dots, a_n b_1, \dots, b_n}(p', l'_i) \prod_{j=1}^n N_{a_j b_j}^{\mu_j \nu_j}(q_j), \quad (6.8)$$

where the primed momentum variables are related to the unprimed ones by Eq. (6.3) and

$$N_{ab}^{\mu\nu}(q) = \Lambda^\mu_{\mu'} \Lambda^\nu_{\nu'} N_{a'b'}^{\mu'\nu'}(q). \quad (6.9)$$

Equation (6.8) follows from the simple observation

$$S F_{\mu_1, \dots, \mu_n \nu_1, \dots, \nu_n}^{a_1, \dots, a_n b_1, \dots, b_n}(p, l_i) S^{-1} \prod_{j=1}^n N_{a_j b_j}^{\mu_j \nu_j}(q_j) = F_{\mu_1, \dots, \mu_n \nu_1, \dots, \nu_n}^{a_1, \dots, a_n b_1, \dots, b_n}(p', l'_i) \prod_{j=1}^n N_{a_j b_j}^{\mu_j \nu_j}(q_j). \quad (6.10)$$

$S_F(p')$, on the other hand, is given by

$$S_F(p') = \sum_F \int \left[\prod_{i=1}^r \frac{d^4 l'_i}{(2\pi)^4} \right] F_{\mu_1, \dots, \mu_n \nu_1, \dots, \nu_n}^{a_1, \dots, a_n b_1, \dots, b_n}(p', l'_i) \prod_{j=1}^n N_{a_j b_j}^{\mu_j \nu_j}(q_j). \quad (6.11)$$

Thus,

$$S_F(p') - SS_F(p)S^{-1} = \sum_F \int \left[\prod_{i=1}^r \frac{d^4 l'_i}{(2\pi)^4} \right] F_{\mu_1, \dots, \mu_n}^{a_1, \dots, a_n, b_1, \dots, b_n}(p', l'_i) \left[\prod_{j=1}^n N_{a_j b_j}^{\mu_j \nu_j}(q'_j) - \prod_{j=1}^n N_{a_j b_j}^{\mu_j \nu_j}(q_j) \right]. \tag{6.12}$$

Note that if we had used a covariant gauge then $N_{ab}^{\mu\nu}(q) = N_{ab}^{\mu\nu}(q')$ and the right-hand side of (6.12) would have vanished. This states the simple fact that in a covariant gauge $S_F(p')$ is identical to $SS_F(p)S^{-1}$.

We have considered an infinitesimal boost along the Z direction and want to keep only first-order terms in β . Since $N^{\mu\nu}(q')$ and $N^{\mu\nu}(q)$ differ from each other by order β we may define

$$N_{ab}^{\mu\nu}(q') - N_{ab}^{\mu\nu}(q) = \beta S_{ab}^{\mu\nu}(q') + O(\beta^2) \tag{6.13}$$

and write the right-hand side of (6.12) as

$$\beta \sum_F \int \left[\prod_{i=1}^r \frac{d^4 l'_i}{(2\pi)^4} \right] F_{\mu_1, \dots, \mu_n}^{a_1, \dots, a_n, b_1, \dots, b_n}(p', l'_i) \sum_{i=1}^n \left[\prod_{j \neq i} N_{a_j b_j}^{\mu_j \nu_j}(q'_j) \right] S_{a_i b_i}^{\mu_i \nu_i}(q'_i) + O(\beta^2). \tag{6.14}$$

The above expression has a nice physical interpretation. Let us define by S gluon a gluon with propagator $S_{ab}^{\mu\nu}(q)/(q^2 + i\epsilon)$. Then expression (6.14) is the sum of all Feynman diagrams where one of the gluons is an S gluon, while all others are the usual axial gauge gluon. The expression for $S_{ab}^{\mu\nu}$ has been derived in Appendix C and is of the form

$$S_{ab}^{\mu\nu}(k) = \delta_{ab} [S^\mu(k)k^\nu + S^\nu(k)k^\mu], \tag{6.15}$$

$S^\mu(k)$ being a vector whose various components are given in Appendix C. Since $S^{\mu\nu}(k)$ is a sum of terms proportional to k^μ or k^ν we may use Ward identities and relations shown in Fig. 7 to sum over all S gluon insertions. The result of the summation has been shown in Fig. 29. The gluons marked S have propagators $S^\mu(k)/(k^2 + i\epsilon)$, μ being the Lorentz index of the uncircled end of the gluon. The rules for the circled vertices are the same as that for the K gluons given in Appendix A; however, the factor $\omega^\mu/(\omega \cdot k + i\epsilon)$ is absent. In order to distinguish these vertices from the K -gluon vertices we shall always mark the S -gluon propagator by S near the circled vertex.

From Eq. (C6) we get

$$S^-(k) = -n^- P \left(\frac{1}{n \cdot k} \right) + \frac{n^-}{2} P \left[\frac{n^- k^+ - n^+ k^-}{(n \cdot k)^2} \right] - \frac{k^-}{2} n^2 P \left[\frac{n^- k^+ - n^+ k^-}{(n \cdot k)^3} \right]. \tag{C6}$$

This shows that in the limit $|k^+| \gg |k^-|$ and $|k_\perp|$, S^- is of the order $(n_\perp \cdot k_\perp)/(k \cdot n)^2$. However, power counting shows that if the S gluon has to be the part of a jet then it must go as $1/(n \cdot k)$, i.e., it should

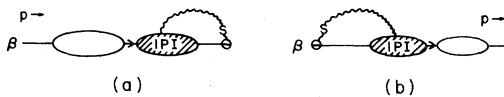


FIG. 29. Sum of all Feynman diagrams in expression (6.14).

not have any numerator suppression factor. This is illustrated by the simple example shown in Fig. 30. If the S gluon is jetlike then in the notation of Ref. 13 each of the lines carrying momenta k and $p-k$ contribute a factor of λ in the denominator. The jet-loop integration gives two powers of λ in the numerator. Hence in order that the integral be logarithmically divergent in the $\lambda \approx 0$ region we should not have any numerator suppression factor. This means that we must have an $S\gamma^+$ term at the gluon-fermion vertex. But Eq. (C6) shows that S^- has a k_T in the numerator which goes as $\lambda^{1/2}$ and destroys the logarithmic divergence at $\lambda=0$. The same argument may be extended to diagrams involving more loops to show that the S gluon can never be collinear to the jet. Hence it must be either contracted or soft.

Now if we compare the right-hand side of Eq. (6.6) with Fig. 29, we immediately see that Fig. 29(a) corresponds to the first term on the right-hand side of (6.6), while Fig. 29(b) corresponds to the second term. From now on we shall deal with the first term only. To analyze Fig. 29(a) we first investigate the behavior of S^μ in various regions in momentum space. As shown above, the contribution from a region where the S gluon is collinear to p is suppressed by a power of $(q^2)^{1/2}$. Hence, we need to consider only those regions where the S gluon is either soft or contracted. We now decompose the uncircled end of the S gluon into G and K terms using Eq. (4.2) with the $i\epsilon$ term replaced by $-i\epsilon$. This is because if we consider a typical diagram contributing to Fig. 29(a) as shown in Fig. 30, the fermion denominator carrying the S -gluon momentum k goes as $1/[(p-k)^2 - m^2 + i\epsilon] = -1/$

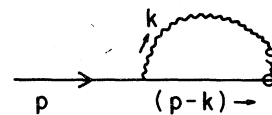


FIG. 30. A typical diagram contributing for Fig. 29(a).

$(2p \cdot k - k^2 - i\epsilon)$. Hence in order that the momentum k^- is not pinched between the Grammer-Yennie denominator and the jet denominators, we must choose the sign of $i\epsilon$ in this particular way. We now sum over all insertions of the K gluon including insertions on the fermion line; as a result we obtain a diagram of the form shown in Fig. 31 (ignoring the diagram which does not have a pole at $p^2 = m^2$). The G term prevents some more lines from being parallel to p (e.g., in Fig. 32 the gluons S_1 and S_2 are prevented from being parallel to p). We now decompose one of these gluons into G and K vertices and sum over all insertions. This process is continued exactly according to the steps I to V of the algorithm, the only difference being that we now sum over insertions on the fermion line also. We stop the process if (1) we get a gluon coupled to the quark line through a G vertex (Fig. 33) or (2) the gluons connected to the S gluon completely decouple from the fermion line and are attached to the rightmost end of the fermion line through circled vertices (Fig. 34).

Let us denote by $f(p)$ the sum of all the diagrams obtained at the end of the decomposition procedure with the self-energy part truncated. Typical contributions to $f(p)$ have been shown in Fig. 35. We may then write

$$\begin{aligned} \{ [Z_2(p')]^{1/2} - [Z_2(p)]^{1/2} \} \frac{i}{\not{p}' - m} [\bar{Z}_2(p')]^{1/2} \\ = \beta f(p) [Z_2(p)]^{1/2} \frac{i}{\not{p}' - m} [\bar{Z}_2(p')]^{1/2} + O(\beta^2). \end{aligned} \quad (6.16)$$

Now $[Z_2(p)]^{1/2}$ and $f(p)$ depend on $p \cdot n$ which is again a function of p^+ . Since $p'^+ = p^+(1 + \beta)$, we may write the left-hand side of the above equation as

$$\beta p^+ \frac{\partial [Z_2(p^+)]^{1/2}}{\partial p^+} \frac{i}{\not{p}' - m} [\bar{Z}_2(p^+)]^{1/2} + O(\beta^2). \quad (6.17)$$

Comparing first-order terms in β from both sides of (6.16) we get

$$p^+ \frac{\partial [Z_2(p^+)]^{1/2}}{\partial p^+} = f(p^+) [Z_2(p^+)]^{1/2}. \quad (6.18)$$

The solution to this equation is



FIG. 31. Sum of all insertions of the K part of the S gluon.

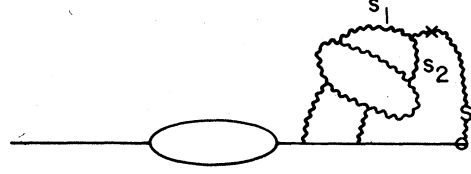


FIG. 32. A typical diagram containing the G part of the S gluon.

$$[Z_2(p)]^{1/2} = B(m_R, \mu, \tau, g) \exp \left[\int^{(q^2)^{1/2}} f(x) \frac{dx}{x} \right]. \quad (6.19)$$

In those diagrams in $f(p)$ which contain a crossed vertex on the fermion line, all lines must carry momentum $\sim (q^2)^{1/2}$ in all components. Diagrams which do not have crossed vertices on the fermion line [e.g., Fig. 35(a)] may have soft divergences; the scale of all the momenta of all the lines is however set by the scale of the momentum of the S gluon. In other words, if in $f(p)$ we integrate over all momenta except for the transverse momentum \vec{k}_T of the S gluon and call this result $\Phi(p^+, \mu, m_R, \tau, \vec{k}_T, g)$, then this has a finite $p^+ \rightarrow \infty$, $m_R \rightarrow 0$, and $\tau \rightarrow 0$ limit for fixed \vec{k}_T , since for fixed \vec{k}_T all the momenta flowing through the diagram are of the order of $|\vec{k}_T|$. We may write

$$f(p^+, \mu, m_R, \tau, g) = \int d^{d-2} k_T \Phi(p^+, \mu, m_R, \tau, \vec{k}_T, g). \quad (6.20)$$

Note that if we replace Φ by its limit as $p^+ \rightarrow \infty$ in (6.20), then the k_T integral will diverge at ∞ , while if we replace Φ by its limit as $m_R, \tau \rightarrow 0$ and replace d by 4 in (6.20), the k_T integral will diverge at zero. Let us break up (6.20) (following Ref. 5)

$$f(p^+, \mu, m_R, \tau, g) = f_1(p^+, \mu, g) + f_2(p^+, \mu, m_R, \tau, g), \quad (6.21)$$

where

$$\begin{aligned} f_1(p^+, \mu, g) = \int d^d k_T \frac{\vec{k}_T^2}{\vec{k}_T^2 + \mu^2} \\ \times \Phi(p^+, \mu, m_R = 0, \tau = 0, \vec{k}_T, g) \end{aligned} \quad (6.22)$$

and

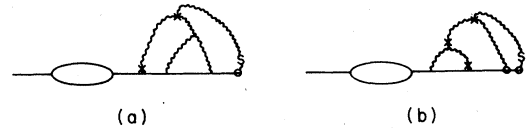


FIG. 33. Typical diagrams obtained at the end of the decomposition procedure with G vertices on the fermion line.

$$f_2(p^*, \mu, m_R, \tau, g) = \int d^4 k_T \left[\Phi(p^*, \mu, m_R, \tau, k_T, g) - \frac{\vec{k}_T^2}{\vec{k}_T^2 + \mu^2} \Phi(p^*, \mu, m_R = 0, \tau = 0, \vec{k}_T, g) \right]. \quad (6.23)$$

The integral in (6.22) is now convergent at $k_T = 0$ due to the extra factor of \vec{k}_T^2 in the numerator. This integral receives contribution from the region $\mu^2 \leq \vec{k}_T^2 \leq q^2$. The integral in (6.23) receives contribution from $\vec{k}_T^2 \leq \mu^2$, m_R^2 since for $\vec{k}_T^2 \gg \mu^2$, m_R^2 we can replace $\Phi(p^*, \mu, m_R, \tau, k_T, g)$ by $\Phi(p^*, \mu, 0, \vec{k}_T, g)$ and $\vec{k}_T^2 / (\vec{k}_T^2 + \mu^2)$ in the second term by unity so that the two terms cancel. Thus if we take $\mu^2 \sim m_R^2$, we may replace p^* by ∞ in (6.23) up to order m_R/p^* and hence f_2 ceases to be a function of p^* .

Also note that although $f(p)$ is superficially ultraviolet divergent by power counting, these divergences must cancel when we sum over all the diagrams contributing to $f(p)$. This is apparent from Eq. (6.18). Hence f_1 is ultraviolet convergent (f_2 is of course ultraviolet convergent). f_2 on the other hand is infrared divergent and blows up in the limit $\tau \rightarrow 0$.

Since f_1 is ultraviolet convergent, it satisfies the renormalization-group equation

$$\left(\mu \frac{\partial}{\partial \mu} + \beta(g) \frac{\partial}{\partial g} \right) f_1(p^*/\mu, g) = \gamma_1(g, p^*/\mu), \quad (6.24)$$

where

$$\gamma_1\left(g, \frac{p^*}{\mu}\right) = - \int d^2 k_T \frac{2\vec{k}_T^2 \mu^2}{(\vec{k}_T^2 + \mu^2)^2} \times \Phi(p^*, \mu, m_R = 0, \tau = 0, \vec{k}_T, g). \quad (6.25)$$

The integral in (6.25) receives contribution only from the region $\vec{k}_T^2 \sim \mu^2$, hence up to order μ/p^* , we may replace $\Phi(p^*, \dots)$ by its limit as $p^* \rightarrow \infty$ in the integrand. The Eq. (6.24) then stands as

$$\left(\mu \frac{\partial}{\partial \mu} + \beta(g) \frac{\partial}{\partial g} \right) f_1(p^*/\mu, g) = \gamma_1(g) \quad (6.26)$$

with

$$\gamma_1(g) = - \int d^2 k_T \frac{2\vec{k}_T^2 \mu^2}{(\vec{k}_T^2 + \mu^2)^2} \times \Phi(p^* = \infty, \mu, m_R = 0, \tau = 0, \vec{k}_T, g). \quad (6.27)$$

The solution to Eq. (6.26) is

$$f_1((q^2)^{1/2}/\mu, g) = - \int_{\mu}^{(q^2)^{1/2}} \frac{d\mu'}{\mu'} \gamma_1(\bar{g}(\mu')) + f_1(1, \bar{g}((q^2)^{1/2})), \quad (6.28)$$

where $\bar{g}(\mu')$ is the running coupling constant defined in Eq. (3.15). Equation (6.19) then gives

$$(Z_2(p))^{1/2} = B(m_R, \mu, \tau, g) \exp \left[\int_{\mu}^{(q^2)^{1/2}} \frac{d(q'^2)^{1/2}}{(q'^2)^{1/2}} \left(- \int_{\mu}^{(q'^2)^{1/2}} \frac{d(q''^2)^{1/2}}{(q''^2)^{1/2}} \gamma_1(\bar{g}((q'^2)^{1/2})) + f_1(1, \bar{g}((q'^2)^{1/2})) + f_2(\infty, \mu, m_R, \tau, g) \right) \right]. \quad (6.29)$$

In lowest-order perturbation expansion $\gamma_1 \sim g^2$. This implies that as $q'^2 \rightarrow \infty$ $\gamma_1(\bar{g}(q'^2)) \sim 1/\ln(q'^2)^{1/2}$. Thus,

$$\int_{\mu}^{(q^2)^{1/2}} \frac{d(q'^2)^{1/2}}{(q'^2)^{1/2}} \int_{\mu}^{(q'^2)^{1/2}} \frac{d(q''^2)^{1/2}}{(q''^2)^{1/2}} \gamma_1(\bar{g}((q'^2)^{1/2})) \sim \int_{\mu}^{(q^2)^{1/2}} \frac{d(q'^2)^{1/2}}{(q'^2)^{1/2}} [\ln \ln(q'^2)^{1/2} + O(1)] \sim [\ln((q^2)^{1/2}) \ln \ln((q^2)^{1/2})] + O[\ln((q^2)^{1/2})]. \quad (6.30)$$

Also

$$\int_{\mu}^{(q^2)^{1/2}} f_1(1, \bar{g}((q'^2)^{1/2})) \frac{d(q'^2)^{1/2}}{(q'^2)^{1/2}} \sim \ln \ln(q^2)^{1/2} \quad (6.31)$$

and

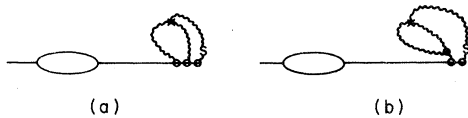


FIG. 34. Typical diagrams obtained at the end of the decomposition procedure with no G vertex on the fermion line.

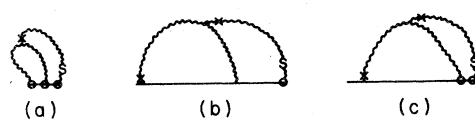


FIG. 35. Typical contributions to $f(p)$.

$$\int_{\mu}^{(q^2)^{1/2}} f_2(\infty, \mu, m_R, \tau, g) \frac{d(q'^2)^{1/2}}{(q'^2)^{1/2}} \sim f_2(\infty, \mu, m_R, \tau, g) \ln(q^2)^{1/2}. \quad (6.32)$$

Note that f_2 is infrared divergent, i.e., it blows up in the limit $\tau \rightarrow 0$. This point has been discussed in the Introduction.

Using Eqs. (4.4), (4.14), and (6.29) we may finally write the Sudakov form factor as

$$\begin{aligned} \bar{u}(p) \epsilon \cdot \gamma v(p') C(m_R, \mu, \tau, g) \exp \left[\int_{\mu}^{(q^2)^{1/2}} \frac{d(q'^2)^{1/2}}{(q'^2)^{1/2}} \left(-2 \int_{\mu}^{(q'^2)^{1/2}} \frac{d(q''^2)^{1/2}}{(q''^2)^{1/2}} \gamma_1(\bar{g}((q'^2)^{1/2})) + 2f_1(1, \bar{g}((q'^2)^{1/2})) \right. \right. \\ \left. \left. + 2f_2(\infty, \mu, m_R, \tau, g) + \chi(\mu, (q'^2)^{1/2}, g) + \chi'(\mu, (q'^2)^{1/2}, g) \right) \right]. \end{aligned} \quad (6.33)$$

Asymptotic behavior of various terms in the exponential has been given in Eqs. (4.15) and (6.30)–(6.32).

From the above discussion it is clear that if we want the coefficient of the leading term in the exponential, we must evaluate $\gamma_1(\bar{g})$ up to lowest order in perturbation theory. This can be done by evaluating the integral on the right-hand side of Eq. (6.27). However there is another way of evaluating this coefficient. Let $\gamma_1(\bar{g}) = a_1 \bar{g}^2 + O(\bar{g}^4)$. Then, noting that in lowest order in g (the fixed coupling constant) $\bar{g} = g$, we get

$$\gamma_1(\bar{g}) = a_1 g^2 + O(g^4). \quad (6.34)$$

Hence

$$\begin{aligned} \int_{\mu}^{(q^2)^{1/2}} \frac{d(q'^2)^{1/2}}{(q'^2)^{1/2}} \int_{\mu}^{(q'^2)^{1/2}} \frac{d(q''^2)^{1/2}}{(q''^2)^{1/2}} \gamma_1(\bar{g}((q'^2)^{1/2})) = a_1 g^2 \frac{1}{2} \ln^2[(q^2)^{1/2}/\mu] \\ + O(g^4) + O(g^2 \ln((q^2)^{1/2}/\mu)), \end{aligned} \quad (6.35)$$

where $O(g^4)$ terms include terms of order g^4 or more multiplied by powers of $\ln[(q^2)^{1/2}/\mu]$ and $O[g^2 \ln((q^2)^{1/2}/\mu)]$ include terms of order $g^2 \ln q^2$. Thus (6.33) shows that in lowest order in g^2 , the form factor may be written as

$$\bar{u}(p) \epsilon \cdot \gamma v(p') C(m_R, \mu, \tau, g) \{1 - a_1 g^2 \ln^2[(q^2)^{1/2}/\mu] + O(g^4) + O(g^2 \ln((q^2)^{1/2}/\mu))\}. \quad (6.36)$$

Explicit one-loop calculation shows that the form factor is given by⁶

$$\bar{u}(p) \epsilon \cdot \gamma v(p') \left[1 - C_F \frac{g^2}{4\pi^2} \ln^2 \frac{(q^2)^{1/2}}{\mu} + O(g^4) + O\left(g^2 \ln \frac{(q^2)^{1/2}}{\mu}\right) \right]. \quad (6.37)$$

Comparing (6.36) with (6.37) we get

$$a_1 = C_F/4\pi^2, \quad (6.38)$$

C_F being the eigenvalue of the Casimir operator in fermion representation. Now for an $SU(N)$ gauge theory with f flavors and fermions in its fundamental representation we have

$$\bar{g}^2 (q^2)^{1/2} = \frac{16\pi^2}{\beta_0 \ln(q^2/\Lambda^2)}, \quad (6.39)$$

where Λ is the strong interaction mass scale and

$$\beta_0 = \frac{11}{3}N - \frac{2}{3}f, \quad (6.40)$$

$$C_F = (N^2 - 1)/2N. \quad (6.41)$$

Hence, in the limit $(q^2)^{1/2} \rightarrow \infty$, the form factor behaves as

$$\begin{aligned} \bar{u}(p) \epsilon \cdot \gamma v(p') C(m_R, \mu, \tau, g) \exp \left\{ -2 \int_{\mu}^{(q^2)^{1/2}} \frac{d(q'^2)^{1/2}}{(q'^2)^{1/2}} \int_{\mu}^{(q'^2)^{1/2}} \frac{d(q''^2)^{1/2}}{(q''^2)^{1/2}} \alpha_1 \frac{8\pi^2}{\beta_0} \frac{1}{\ln[(q'^2)^{1/2}/\Lambda]} + O(\ln(q^2)^{1/2}) \right\} \\ \sim \bar{u}(p) \epsilon \cdot \gamma v(p') C(m_R, \mu, \tau, g) \exp \left[-\frac{16\pi^2 a_1}{\beta_0} \ln \frac{(q^2)^{1/2}}{\mu} \ln \ln \frac{(q^2)^{1/2}}{\mu} + O\left(\ln \frac{(q^2)^{1/2}}{\mu}\right) \right]. \end{aligned} \quad (6.42)$$

Since a_1 and β_0 are both positive numbers, the above equation shows that the form factor decreases to zero in the limit $q^2 \rightarrow \infty$.

VII. CONCLUSION

In this article we have found a systematic way to study the behavior of the fermion form factor in non-Abelian gauge theories in the limit of very large momentum transfer and the fermion lines on shell. We have summed all terms of order $(g^2)^n [\ln((q^2)^{1/2}/m)]^n$ but ignored terms which are suppressed by a power of $m/(q^2)^{1/2}$. The form factor calculated this way decreases as

$$\exp\left(-\frac{16\pi^2 a_1}{\beta_0} \ln \frac{(q^2)^{1/2}}{\mu} \ln \ln \frac{(q^2)^{1/2}}{\mu}\right)$$

in the limit $(q^2)^{1/2} \rightarrow \infty$.

The full result is given in Eq. (6.33).

ACKNOWLEDGMENTS

I wish to thank George Sterman and Sunil Mukhi for many helpful discussions and for reading the manuscript. This work was supported in part by the National Science Foundation Grant No. PHY79-06376A01.

APPENDIX A: EXPRESSION FOR SOME SPECIAL VERTICES USED IN THE TEXT

$$\begin{aligned} \text{Diagram 1} &= \omega^\mu k^\nu / \omega.k \\ \text{Diagram 2} &= i f_{abc} (\omega^\rho / \omega.k) g^{\mu\nu} \\ \text{Diagram 3} &= (\omega^\mu / \omega.k) (T_C)_{ij} \\ \text{Diagram 4} &= -(\omega^\mu / \omega.k) (T_C)_{ij} \end{aligned} \tag{A1}$$

APPENDIX B: "COMPOSITE" THREE-POINT VERTICES

In this appendix we shall show that if we have a soft G gluon attached to a jet line through a "composite" three-point vertex then we shall get the same suppression factor as we would if the G gluon had been attached to the jet line through an

elementary (bare) three-point vertex. Here by "composite" three-point vertex we mean vertices that may appear as subdiagrams in graphs contributing to the constants $\lambda_0, \lambda_1, \dots$, and ψ_0, ψ_1, \dots , in Sec. IV. This result is needed in order to show that for the graphs contributing to the λ 's and ψ 's, all the internal lines are really constrained to carry UV momenta, so that $(q^2)^{1/2}$ and μ are the only mass parameters on which these quantities may depend. Examples of such composite three-point vertices have been shown in Fig. 36. The incoming and outgoing jet lines are shown by thick lines in these figures.

First we shall show that all lines inside a composite three-point vertex carry ultraviolet momentum. We shall prove this for an $(N+1)$ -loop composite vertex assuming that an N -loop composite three-point G vertex gives the same suppression factor as a bare G vertex. Then in an $(N+1)$ -loop diagram all internal composite three-point G vertices have less than $(N+1)$ loops and hence give the same suppression factor as a bare three-point vertex. But as we have seen in Sec. IV the Grammer-Yennie decomposition is carried out in such a way that none of the internal lines inside a composite vertex can be soft or collinear unless the presence of composite three-point G vertices upsets the power counting. Thus in an $(N+1)$ -loop composite vertex all internal lines carry ultraviolet momenta. This may be illustrated by considering Fig. 36(c). Let us consider a region where S_1, S_2, S_5 , and S_6 are soft while S_3 and S_4 are contracted. Naive power counting indicates a logarithmic divergence from such a region. However, the composite three-point vertex through which the gluon S_1 is attached to the jet line gives an extra suppression factor according to our assumption. Hence contribution from such a region is suppressed. The only region which contributes to this graph in leading power in q^2 is where all internal gluon lines carry large off-shell momenta. This implies that the vertex function is independent of the external soft momentum and also the minus and trasverse components of momenta of the external jet lines.

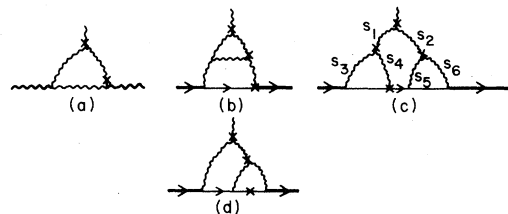


FIG. 36. Examples of composite three-point vertices which appear in the graphs contributing to the ψ 's and λ 's in Eq. (4.18) of the text.

We shall now show that a composite soft G gluon-fermion vertex gives the same suppression factor as the bare vertex. Let ϵ be the polarization vector of the external gluon, K be its momentum, and P and $P+K$ be the momenta of the external jet lines. Let us define the vector R as $\frac{1}{2}(P^*, 0, 0, P^*)$. Then in the leading power approximation the vertex function is a function of ϵ , n , ω , and R . This is true even if we have a crossed fermion line since the $\partial/\partial \ln p^*$ operation is equivalent to an $R \cdot \gamma$ vertex insertion on the fermion line. The function must be invariant under scaling of n and ω . Then since the external gluon couples to the graph through a G vertex, we have $\epsilon \cdot \omega = \epsilon \cdot R = 0$ and the only possible structure of the vertex which does not give the extra suppression factor is of the form

$$\frac{\epsilon \cdot n n \cdot \gamma}{n^2} \times \text{logs of } (P^*/\mu). \quad (\text{B1})$$

Now, any diagram contributing to the vertex will have a string of γ matrices on the fermion line and this is multiplied by a function of ω , n , R , and ϵ . Let us denote this term by $\gamma_{\mu_1} \cdots \gamma_{\mu_r} A^{\mu_1 \cdots \mu_r}(\omega, n, \epsilon, R)$. Now suppose the rightmost vertex on the fermion line (the vertex which produces γ^{μ_1}) is a G vertex [e.g., Fig. 36(b)]. As seen from Eq. (4.2), $G^T \omega_\mu = 0$. Hence if we contract $A^{\mu_1 \cdots \mu_r}$ with ω_{μ_1} , we must get zero. Now $\omega \cdot \omega$, $\omega \cdot \epsilon$, and $\omega \cdot R$ are all zero but $\omega \cdot n$ is not zero. Hence $A^{\mu_1 \cdots \mu_r}$ must be proportional to some linear combination of ω^{μ_1} , ϵ^{μ_1} , and R^{μ_1} but not to n^{μ_1} or $g^{\mu_1 \mu_i}$ ($i=2, \dots, n$). If it is proportional to some linear combination of ω^{μ_1} , R^{μ_1} then $\gamma^{\mu_1} A^{\mu_1 \cdots \mu_r} \gamma_{\mu_1} \cdots \gamma_{\mu_r}$ will be equal to zero since $\omega \cdot \gamma$ and $R \cdot \gamma$ are both proportional to γ^{μ_1} ; this is incompatible with the form given in Eq. (B1). Thus the only possible form of the vertex which may be reduced to the form given in Eq. (B1) is the one where $A^{\mu_1 \cdots \mu_r}$ is proportional to ϵ^{μ_1} . Now since the vertex function is independent of m in leading power in $(q^2)^{1/2}$, we may set m to be zero. Then we shall get a γ matrix from each fermion numerator and each gluon fermion vertex. As a result we must have an odd number of γ matrices on the fermion line, i.e., r must be odd. γ_{μ_1} is contracted with ϵ^{μ_1} . $A^{\mu_1 \mu_2 \cdots \mu_r} \gamma_{\mu_2} \cdots \gamma_{\mu_r}$ contains a product of even number of γ matrices. After reducing the product using γ matrix anticommutation relations and using the fact that $R \cdot \gamma = (P^*/2)\omega \cdot \gamma$, we may bring the product in the form $\epsilon^{\mu_1}(a + bn \cdot \gamma \omega \cdot \gamma)$, where a and b are two scalar functions. Thus the vertex has the form

$$\epsilon \cdot \gamma (a + bn \cdot \gamma \omega \cdot \gamma), \quad (\text{B2})$$

which carries the same suppression factor as we would have obtained if the external G gluon had been attached to the jet through a simple $\epsilon \cdot \gamma$ ver-

tex. This is because the second term satisfies the condition $\epsilon \cdot \gamma n \cdot \gamma \omega \cdot \gamma \gamma^{\mu_1} = 0$, so that we cannot get a $P^* \gamma^{\mu_1}$ factor from the jet numerator sitting next to the vertex.

The same argument holds if the leftmost vertex on the fermion line is a G vertex rather than the rightmost one. If neither the leftmost nor the rightmost vertex is a crossed vertex [e.g., Figs. 36(c) and 36(d)], then we proceed in the following way. We identify the gluon lines attached to the fermion line to the right of the rightmost G vertex or the crossed fermion line, as the case may be. We break up these gluons one by one into G and K gluons and sum over all insertions of the K gluons on the fermion line to the right of the G vertex (or the crossed fermion line). As a result we get various types of diagrams. In one class of diagrams we shall have one or more gluons attached to the rightmost end of the fermion line through circled vertices; such diagrams are suppressed by a power of P^* since they remove an external jet line from the diagram. We also have diagrams where all gluons to the right of the rightmost crossed vertex (or the $R \cdot \gamma$ vertex generated by $p^* \partial/\partial p^*$ operation) are attached just to the right of this vertex through circled vertices (as shown in Fig. 37). In these the rightmost vertex on the fermion line is again a crossed vertex or a vertex proportional to $R \cdot \gamma$ (circled vertices do not have any Dirac structure), and we may show in the same way as before that this carries the same suppression factor as the case when the external G gluon is directly attached to the jet line through an elementary three-point vertex proportional to $\epsilon \cdot \gamma$. There are also diagrams involving G gluons; these give rise to new crossed vertices on the fermion line. The process of decomposition into G and K gluons is continued until the rightmost vertex on the fermion line is a crossed vertex. This way we can show that we always get the required suppression factor from a composite three-point jet fermion-soft G -gluon vertex.

Let us now turn to the three-gluon vertex where two of the gluons carry jetlike momenta and one of them carries soft momentum. Let ϵ , ϵ_1 , and ϵ_2 be the polarization vectors of the soft gluon and the two

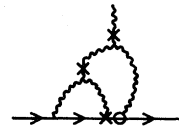


FIG. 37. A typical diagram obtained during the decomposition of a composite three-point jet fermion-soft- G -gluon vertex according to the procedure mentioned in the text.

jet gluons, respectively, and $K, P,$ and $P + K$ be the momenta carried by the soft gluon and the two jet gluons, respectively. As before the vertex function will be independent of $P_1, P,$ and K in leading power approximation. The possible structure of the vertex which does not give the required G -gluon suppression factor is of the form

$$\epsilon_1 \cdot \epsilon_2 (\epsilon \cdot nm \cdot P/n^2) \times \text{logs of } P^+/\mu. \tag{B3}$$

To show that such terms cannot be present in the actual vertex function, let us first note that in any graph contributing to the vertex function all the internal lines are constrained to carry momentum of order P^+ ; hence the vertex is free of infrared divergences. Later we shall express the vertex function as a sum of terms each of which is IR divergent. Such divergences may be regulated by dimensional regularization and must cancel in the sum over all graphs. With this in mind we start undoing the Grammer-Yennie decomposition for the internal vertices in an order exactly opposite to the one in which they were decomposed. At the end of this procedure we shall get three types of diagrams: (1) where all the internal vertices are ordinary vertices [e.g., Fig. 38(a)], (2) where some of the gluon lines are attached to the rightmost or the leftmost points of the jet gluon line through circled vertices [e.g., Fig. 38(b)] and (3) where all the gluon lines attached to the jet gluon are attached to a single point [Fig. 38(c)]. Contributions from class 2 diagrams from the region in momentum-space integration where all the internal momenta are off shell ($\sim P^+$) are suppressed since we lose an external jet denominator in such a diagram. Note that such diagrams may give nonsuppressed contribution from the region where the internal momenta are soft but such contributions must vanish in the sum over all graphs. Contributions from class 3 diagrams, apparently, are not suppressed. The total contribution from such diagrams may be abstractly represented as in Fig. 39, where B is some blob containing crossed as well as ordinary internal vertices. As we shall see, the precise form for B is not required for our purpose. Class 1 diagrams give the same suppression factors as that of soft G gluon attached directly to the jet line. To see this let us note that if $\Gamma_{\mu\nu\rho}$ be the three-gluon vertex, with ρ being

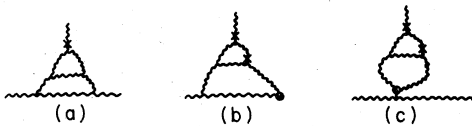


FIG. 38. Typical diagrams obtained as we undo the Grammer-Yennie decomposition for a composite three-point jet gluon-soft- G -gluon vertex.

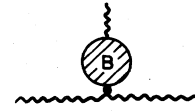


FIG. 39. Abstract representation of the sum of all diagrams of the form Fig. 38(c).

the Lorentz index of the soft gluon, we may write

$$\Gamma_{\mu\nu\rho}(n, P) = \frac{\partial}{\partial P^\rho} \Sigma_{\mu\nu}(n, P), \tag{B4}$$

where $\Sigma_{\mu\nu}$ is the two-point one-particle-irreducible gluon-gluon Green's function. For convenience we have omitted the color indices. In order to get a form (B3) of the vertex function from (B4), we need a term in $\Sigma_{\mu\nu}$ of the form

$$g_{\mu\nu}(n \cdot P)^2 \times \text{logs of } (n \cdot P/\mu). \tag{B5}$$

Absence of such terms in Σ may be shown by the method of induction. We shall assume that the result is true for r -loop diagrams and then show that it is also true for $(r + 1)$ -loop diagrams. Let P' be related to P by an infinitesimal Lorentz boost β along Z direction [Eq. (6.3)] and let us denote by $\delta\Sigma_{\mu\nu}$ the difference $\Sigma_{\mu\nu}(P') - \Sigma_{\mu\nu}(P)$ where $\Sigma'_{\mu\nu}(P)$ and $\Sigma_{\mu\nu}(P)$ are related to each other by the infinitesimal Lorentz transformation considered in Sec. VI. Following the same procedure as in Sec. VI, we may express $\delta\Sigma$ as a sum of diagrams with one internal S gluon and all other ordinary gluons. Remembering that Σ is a sum over all one-particle-irreducible diagrams only, the term $[-iN/(P^2 + i\epsilon)]\delta\Sigma[-iN/(P^2 + i\epsilon)]$ may be expressed as a sum of diagrams shown in Fig. 40. [Here N represents the matrix $N^{\mu\nu}(P)$]. Since $g_{\mu\nu}$ is an invariant tensor, $\Sigma_{\mu\nu}(P') - \Sigma'_{\mu\nu}(P)$ according to the expression (B5) for Σ , should go as $g_{\mu\nu}(P^+)^2 \times \text{logs of } (P^+/\mu)$. Hence $(-iN/P^2)\delta\Sigma(-iN/P^2)$ should go as $(P^+)^2(P^2)^{-2}NN$. This has two jet denominators and no numerator suppression factor. On the other hand, if we look at Figs. 40, the first two have only one jet denominator each. Figures 40(c) and 40(d) apparently have two jet denominators each. But the Σ 's involved in these graphs have less loops than the original graph and hence by assumption cannot contain a term of the form given in expression (B5). Any other form for Σ would necessarily give an extra suppression factor. n contracted with N will give zero, while P contrac-

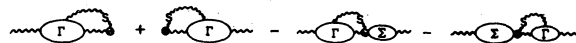


FIG. 40. Diagrammatic expression for $\beta^{-1}(-iN/P^2) \times \delta\Sigma(-iN/P^2)$.

ted with N will kill the P^2 pole in the denominator and hence give a suppression. Thus terms of the form $n^\mu n^\nu$, $P^\mu P^\nu$, $N^\mu P^\nu$, or $N^\nu P^\mu$ in $\Sigma^{\mu\nu}$ will give a suppressed contribution. A term of the form $g^{\mu\nu} P^2$ will kill the P^2 pole in the denominator of N/P^2 . Thus the form of $\Sigma_{\mu\nu}$ given in expression (B5) in $(r+1)$ -loop order is inconsistent with the absence of such terms in $\Sigma_{\mu\nu}$ in r -loop order. Since $\Sigma_{\mu\nu}$ is zero at the tree level, we see by induction that a term of the form (B5) is absent in $\Sigma_{\mu\nu}$ in all orders in perturbation theory.

Thus it now remains to be seen that the contribution from diagrams shown in Fig. 39 is suppressed. This will be shown by comparing the three-gluon vertex with the soft-gluon-jet fermion vertex which has already been analyzed. The latter vertex may also be analyzed as the three-gluon vertex. Diagrams of the type shown in Fig. 38 will be present, with the jet gluon line replaced by the jet fermion line. Diagrams of the type Fig. 38(b) may be thrown away by the same reasoning as for the jet gluon line. The sum of diagrams of the form Fig. 38(c) may again be represented in the abstract form shown in Fig. 39. The sum of the diagrams of the type shown in Fig. 38(a) with the jet gluon replaced by the jet fermion line may be expressed as

$$\Gamma_\rho = \frac{\partial}{\partial P^\rho} \Sigma(P), \quad (\text{B6})$$

where Γ_ρ is the gluon-fermion vertex and Σ is the sum of all one-particle-irreducible fermion self-energy graphs. In order to get a contribution to Γ_ρ of the form given in Eq. (B1), $\Sigma(P)$ must have a term of the form

$$(n \cdot \gamma n \cdot P / n^2) \times \text{logs of } (P \cdot n / \mu). \quad (\text{B7})$$

Absence of such terms in $\Sigma(P)$ may be shown by considering the difference $\Sigma(P') - S\Sigma(P)S^{-1}$, where P' and P are related by Eq. (6.3) and S is defined by Eq. (6.5). If we call this difference $\delta\Sigma$ then according to (B7), $\delta\Sigma$ will contain a term proportional to $\gamma^* P^* \times \text{logs of } (P \cdot n / \mu)$. Thus if we consider the expression $[i/(\not{P} - m)]\delta\Sigma[i/(\not{P} - m)]$ it should go as $P^* \gamma^* P^* \gamma^* P^* \gamma^* / (P^2 - m^2)^2 \sim \gamma^* \gamma^* \gamma^* (P^*)^3 \times (P^2 - m^2)^{-2}$. Thus this contains two jet denominators and no numerator suppression factor. On the other hand, $[i/(\not{P} - m)]\delta\Sigma[i/(\not{P} - m)]$ may be expressed as the sum of diagrams of the form shown in Fig. 40, with the jet gluon replaced by jet fermion, $\Gamma_{\mu\nu\rho}$ replaced by Γ_ρ and $\Sigma_{\mu\nu}$ replaced by Σ . The same type of analysis shows that none of these figures can produce two jet denominators without any numerator suppression factor, if we assume that terms of the form given in expression (B7) are absent from Σ in lower loop orders. This shows by induction that up to all orders of perturbation

theory terms of the form given in expression (B7) are absent from Σ since they are absent from Σ at the tree level.

[The above result has one important consequence. In the limit $n \cdot P \gg m$, the only other possible term in Σ is of the form $P \times \text{logs of } (P^* / \mu)$. Thus in this limit the full fermion propagator behaves as $(i/\not{P}) \times \text{logs of } (P^* / \mu)$. This shows that the fermion wave-function renormalization constant reduces to identity matrix in Dirac space in the limit $n \cdot p \gg m$ as assumed in the text.]

Thus for both the three-gluon and the gluon-fermion vertex, we are left with the diagrams of the type shown in Fig. 39. However, we have already seen that the total contribution from a fermion-soft-G-gluon vertex is suppressed. Thus the blob B in Fig. 39 must carry a suppression factor when the external jet is a fermion line, but since the blob B is independent of whether we have fermion or gluon lines in the external jet, the same suppression factor must be present for jet gluon lines as well. Hence contributions from all the diagrams shown in Fig. 38 are suppressed.

We have thus proved that if a soft G gluon is attached to a jet fermion or a jet gluon line through a composite three-point vertex we get the same suppression factor as the case when the composite vertex is replaced by the elementary vertex.

APPENDIX C: THE S GLUON

As defined in the text [Eq. (6.13)]

$$\beta S_{ab}^{\mu\nu}(q') = N_{ab}^{\mu\nu}(q') - N_{ab}'^{\mu\nu}(q), \quad (\text{C1})$$

where q' and q are related by Eq. (6.3) of the text. Using Eq. (2.2), we get

$$S_{ab}^{\mu\nu}(k') = \delta_{ab}(S^\mu k'^\nu + S^\nu k'^\mu), \quad (\text{C2})$$

where

$$\beta S^\mu(k') = P \frac{n'^\mu}{k \cdot n} - P \frac{n^\mu}{k' \cdot n} + \frac{n^2}{2} k'^\mu P \left(\frac{1}{k' \cdot n} \right)^2 - \frac{n^2}{2} k'^\mu P \left(\frac{1}{k \cdot n} \right)^2. \quad (\text{C3})$$

If we denote by δn and δk the vectors $n' - n$ and $k' - k$ and if we keep only up to first-order terms in β , the above equation may be written as

$$\beta S^\mu = \delta n^\mu P(1/k \cdot n) + n^\mu P \left(\frac{n \cdot \delta k}{(k \cdot n)^2} \right) - k^\mu n^2 P \left(\frac{n \cdot \delta k}{(k \cdot n)^3} \right). \quad (\text{C4})$$

Using Eqs. (6.3) we may evaluate various components of S . They are

$$S^+ = P\left(\frac{n^+}{k \cdot n}\right) + \frac{n^+}{2} P\left(\frac{n^- k^+ - n^+ k^-}{(k \cdot n)^2}\right) - \frac{k^-}{2} n^2 P\left(\frac{n^- k^+ - n^+ k^-}{(k \cdot n)^3}\right), \quad (C6)$$

$$- \frac{k^+}{2} n^2 P\left(\frac{n^- k^+ - n^+ k^-}{(k \cdot n)^3}\right), \quad (C5)$$

$$S^i = \frac{n^i}{2} P\left(\frac{n^- k^+ - n^+ k^-}{(k \cdot n)^2}\right)$$

$$S^- = -n^- P\left(\frac{1}{k \cdot n}\right) + \frac{n^-}{2} P\left(\frac{n^- k^+ - n^+ k^-}{(k \cdot n)^2}\right) - \frac{k^i}{2} n^2 P\left(\frac{n^- k^+ - n^+ k^-}{(k \cdot n)^3}\right) \quad (i=1, 2). \quad (C7)$$

¹V. Sudakov, Zh. Eksp. Teor. Fiz. 30, 87 (1956) [Sov. Phys.—JETP 3, 65 (1956)].

²R. Jackiw, Ann. Phys. (N.Y.) 48, 292 (1968).

³Paul M. Fishbane and J. D. Sullivan, Phys. Rev. D 4, 458 (1971).

⁴A. H. Mueller, Phys. Rev. D 20, 2037 (1979).

⁵J. C. Collins, Phys. Rev. D 22, 1478 (1980).

⁶J. M. Cornwall and G. Tiktopoulos, Phys. Rev. D 13, 3370 (1976).

⁷H. D. Dahmen and F. Steiner, DESY Report No. 80/37, 1980 (unpublished).

⁸V. V. Belokurov and N. J. Ussyukina, Phys. Lett. 94B, 251 (1980).

⁹D. Amati, A. Bassetto, M. Ciafaloni, G. Marchesini, and G. Veneziano, Nucl. Phys. B173, 429 (1980).

¹⁰R. Gastmans and R. Meuldermans, Nucl. Phys. B63, 277 (1973); W. Marciano and A. Sirlin, *ibid.* B88, 86

(1975); R. Gastmans, J. Verwaest, and R. Meuldermans, *ibid.* B105, 454 (1976).

¹¹V. Ganapathi and G. Sterman, Phys. Rev. D 23, 2408 (1981).

¹²G. 't Hooft, Nucl. Phys. B61, 455 (1973).

¹³G. Sterman, Phys. Rev. D 17, 2773 (1978).

¹⁴G. Grammer and D. R. Yennie, Phys. Rev. D 8, 4332 (1973). See also S. Libby and G. Sterman, Phys. Rev. D 18, 3252 (1978) and Ref. 5. For modification of this technique for QCD, see J. C. Collins and G. Sterman, Nucl. Phys. B185, 172 (1981).

¹⁵J. C. Collins and D. E. Soper, Oregon Report No. OITS 155, 1981 (unpublished).

¹⁶J. Frenkel and J. C. Taylor, Nucl. Phys. B116, 185 (1976).

¹⁷A. L. Mason, Nucl. Phys. B104, 141 (1976).